

Arithmeticity and hidden symmetries of fully augmented pretzel link complements

Jeffrey S. Meyer, Christian Millichap
and Rolland Trapp

ABSTRACT. This paper examines number theoretic and topological properties of fully augmented pretzel link complements. In particular, we determine exactly when these link complements are arithmetic and exactly which are commensurable with one another. We show these link complements realize infinitely many CM-fields as invariant trace fields, which we explicitly compute. Further, we construct two infinite families of non-arithmetic fully augmented link complements: one that has no hidden symmetries and the other where the number of hidden symmetries grows linearly with volume. This second family realizes the maximal growth rate for the number of hidden symmetries relative to volume for non-arithmetic hyperbolic 3-manifolds. Our work requires a careful analysis of the geometry of these link complements, including their cusp shapes and totally geodesic surfaces inside of these manifolds.

CONTENTS

1. Introduction	1
2. Geometric decomposition of fully augmented pretzel links	6
3. Hyperbolic reflection orbifolds	15
4. Cusp and trace fields	16
5. Arithmeticity	18
6. Symmetries and hidden symmetries	21
7. Half-twist partners with many hidden symmetries	25
References	32

1. Introduction

Every link $L \subset \mathbb{S}^3$ determines a link complement, that is, a non-compact 3-manifold $M = \mathbb{S}^3 \setminus L$. If M admits a metric of constant curvature -1 , we say that both M and L are hyperbolic, and in fact, if such a hyperbolic

2010 *Mathematics Subject Classification.* Primary: 57M25; Secondary: 57M27, 57M50.
Key words and phrases. hyperbolic link complement, arithmetic link, hidden symmetry.

structure exists, then it is unique (up to isometry) by Mostow–Prasad rigidity. Ever since the seminal work of Thurston in the early 1980s [34], we have known that links are frequently hyperbolic and a significant amount of research has been dedicated to understanding how their geometries relate to topological, combinatorial, and number theoretic properties of these links. In this paper, we further investigate these relationships for a particularly tractable class of links known as *fully augmented links* (FALs). These links often admit hyperbolic structures that can be explicitly described in terms of combinatorial information coming from their respective link diagrams. See Figure 1 for two diagrams of FALs.

There has already been significant progress made in developing relationships between a FAL diagram and the geometry of the corresponding link complement. Geometric structures for these link complements that can be constructed via diagrams were first described by Agol and Thurston in the appendix of [18] in 2004. Futer–Purcell used this construction to determine diagrammatic conditions that guarantee a FAL is hyperbolic and computed explicit estimates on the geometry of the cusp shapes of FALs in [14]. One nice feature of hyperbolic FALs is that any hyperbolic link $L \subset \mathbb{S}^3$ can be constructed via Dehn surgery on a hyperbolic FAL. Futer–Purcell [14] exploited this relationship along with their cusp geometry estimates of FALs to show that highly twisted links coming from Dehn surgeries of FALs admit no exceptional surgeries. Purcell also exploited these geometric structures on FALs in [31] to determine explicit bounds on volumes and cusp volumes of hyperbolic FALs in terms of diagrammatic information. Since the mid 2000s, FALs and their generalizations have further been explored by Purcell [30] & [29], Flint [12], and Harnois–Olson–Trapp [15].

Here, we address several open questions about number theoretic properties and commensurability classes of FALs in the context of *fully augmented pretzel links* (pretzel FALs). These links are an infinite subclass of FALs whose geometric decompositions admit additional properties that can be exploited. They are constructed by fully augmenting any pretzel link, that is, enclosing each twist region of a pretzel link with an unkotted circle, which we call a crossing circle, and removing all full-twists from each twist region. See Figure 1 for a diagram of a pretzel link K and the corresponding pretzel FAL \mathcal{F} . We let \mathcal{P}_n denote a pretzel FAL with n crossing circles and with no twists going through any of the crossing circles. A diagram of \mathcal{P}_3 is depicted on the right side of Figure 1. We set $M_n = \mathbb{S}^3 \setminus \mathcal{P}_n$. We refer to a pair of pretzel FALs as *half-twist partners* if they have the same number of crossing circles and differ by some number of half-twists going through these crossing circles; we also refer to the corresponding link complements as half-twist partners. For instance, \mathcal{F} and \mathcal{P}_3 in Figure 1 are half-twist partners. Half-twist partners frequently exhibit a number of common features, as we shall see in this paper. Moving forward, we will assume that $n \geq 3$, which guarantees that M_n and all of its half-twist partners are hyperbolic.

We refer the reader to Section 2 for a more thorough description of pretzel FALs, their geometric decompositions, and their half-twist partners.

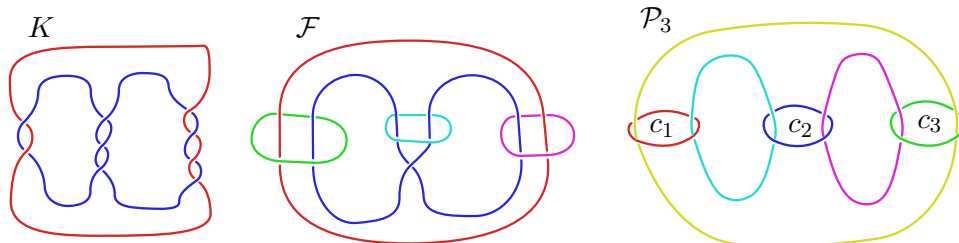


FIGURE 1. On the left is a diagram of a pretzel link K with three twist regions. The middle diagram shows the pretzel FAL \mathcal{F} obtained from fully augmenting K . The right diagram shows the pretzel FAL \mathcal{P}_3 , which is a half-twist partner to \mathcal{F} . Crossing circles of \mathcal{P}_3 are labeled by c_i , for $i = 1, 2, 3$.

Our first major result is a complete classification of which pretzel FAL complements are arithmetic. A link complement is *arithmetic* if its fundamental group is commensurable to $\mathrm{PSL}_2(\mathcal{O}_k)$, where k is some imaginary quadratic extension of \mathbb{Q} and \mathcal{O}_k is its ring of integers. For more on arithmetic 3-manifolds, we refer the reader to [20]. Arithmetic link complements have very restrictive topological and geometric properties, and in particular, they can not contain closed geodesics that are very short; see Theorem 5.1 for an exact description. We show that most pretzel FAL complements (along with their half-twist partners and an even more general type of partner - see Definition 2.4) are non-arithmetic by using their geometric decompositions to find short geodesics. The remaining cases are dealt with by examining properties of the invariant trace fields for these link complements. The following theorem shows that a pretzel FAL complement is non-arithmetic exactly when it has at least 5 crossing circles in its respective diagram. See Section 5 for more details.

Theorem 1.1. *M_n and all of its half-twist partners are arithmetic if and only if $n = 3, 4$.*

In Remark 5.3 we highlight the curious case of M_6 , whose arithmetic and geometric features resemble that of an arithmetic link complement, yet itself is not arithmetic. As mentioned in the previous paragraph, part of the proof of Theorem 1.1 requires comparing invariant trace fields of pretzel FAL complements. The *invariant trace field* of a hyperbolic 3-manifold $M = \mathbb{H}^3/\Gamma$ is the field generated by the traces of the products of squares of elements in Γ . Determining which fields are realized as invariant trace fields of hyperbolic link complements is a question of interest. Neumann has conjectured [25] that every non-real number field arises as the invariant trace field of some hyperbolic 3-manifold, yet to date, a relatively small collection of such fields have been verified to arise in this way.

The invariant trace fields of arithmetic hyperbolic 3-manifolds are well understood [20, Theorem 8.3.2], and by cutting and gluing along thrice punctured spheres, any non-real multi-quadratic extension of \mathbb{Q} can be realized [20, Theorem 5.6.4]. Recently Champanerkar-Kofman-Purcell, assuming a conjecture of Milnor, produced infinitely many incommensurable link complements each with invariant trace field $\mathbb{Q}(i, \sqrt{3})$ [8]. For certain subclasses of hyperbolic 3-manifolds, there are results restricting which invariant trace fields might arise (e.g. as for once-punctured torus bundles [7, Thm. A] or two-bridge knot complements [32, Prop. 2.5]) or providing alternate characterizations (e.g. as for link complements [27, Prop. 4.3]).

Here, we are able to give an explicit description of the invariant trace fields of pretzel FAL complements by analyzing their cusp geometry. The work of Flint [12] implies that the invariant trace field of a FAL complement is the same as its cusp field, that is, the field generated by all the cusp shapes of this link complement. In Section 2.4, we compute the cusp shapes of these link complements and in Section 4 we analyze the properties of their invariant trace fields. The following theorem summarizes the major results from Section 4.

Theorem 1.2. *The invariant trace field of any pretzel FAL with n crossing circles is exactly $\mathbb{Q}(\cos(\pi/n)i)$. In addition, there are only finitely many pretzel FAL complements with the same invariant trace field.*

These fields are particularly nice in that they are imaginary quadratic extensions of totally real number fields (i.e. CM-fields). As of writing this, we are unaware of other hyperbolic 3-manifolds with these as their invariant trace fields for $n \neq 3, 4, 6$. Additionally, as n increases, the number of half-twist partners increases, thereby producing large collections of non-isometric manifolds realizing these invariants.

Our next major result examines commensurability classes of pretzel FAL complements. We say that two manifolds are *commensurable* if they share a common finite-sheeted cover. The *commensurability class* of a manifold M is the set of all manifolds commensurable with M . It is usually difficult to determine if two hyperbolic 3-manifolds are in the same commensurability class. Here, we determine exactly when two pretzel FAL complements are commensurable with each other in terms of the number of crossing circles. To achieve this goal, we rely on a fundamental result of Margulis [21] which implies that if a hyperbolic 3-manifold is non-arithmetic, then there exists a unique minimal orbifold in its commensurability class. For a non-arithmetic M_n , we show that its minimal orbifold \mathcal{O}_n is just the quotient of M_n by a group of symmetries that are visually obvious in a particular diagram for these links; see Section 6 and Figure 12. From here, we compute and compare the volumes of these minimal orbifolds, which help distinguish commensurability classes. We also determine commensurability relations

for half-twist partners via a lemma from Chesebro–Deblois–Wilton [11]. Finally, we deal with the few arithmetic pretzel FAL complements determined by Theorem 1.1 on a case-by-case basis.

Theorem 1.3. *Suppose M and N are two hyperbolic pretzel FAL complements. Then M and N are commensurable if and only if they have the exact same number of crossing circles.*

An essential part of the proof of Theorem 1.3 is showing that the minimal orbifold \mathcal{O}_n is just the quotient of M_n by a group of symmetries. In general, the minimal orbifold \mathcal{O} in the commensurability class of a non-arithmetic hyperbolic 3-manifold $M = \mathbb{H}^3/\Gamma$ is $\mathcal{O} = \mathbb{H}^3/C(\Gamma)$, where $C(\Gamma) = \{g \in \text{Isom}(\mathbb{H}^3) : |\Gamma : \Gamma \cap g\Gamma g^{-1}| < \infty\}$ denotes the commensurator of Γ . Note that, $\Gamma \subset N(\Gamma) \subset C(\Gamma)$, where $N(\Gamma)$ denotes the normalizer of Γ . Elements of $N(\Gamma)/\Gamma$ correspond with symmetries of M , while elements of $C(\Gamma)/N(\Gamma)$ correspond with what we call *hidden symmetries* of M . Thus, our proof of Theorem 1.3 required us to show that M_n has no hidden symmetries. This task is accomplished by showing that if M_n did have hidden symmetries, then \mathcal{O}_n would be a low volume, single-cusped, hyperbolic 3-orbifold. Such orbifolds are either arithmetic or have very specific cusp shapes. In Section 2.4, the necessary cusp shape analysis is provided to help eliminate the possibility of M_n having hidden symmetries.

Margulis’s work [21] mentioned above can also be stated as a classification of arithmetic manifolds in terms of hidden symmetries: a hyperbolic 3-manifold is arithmetic if and only if it has an infinite number of hidden symmetries. Thus, it is natural to ask: how many hidden symmetries could a non-arithmetic hyperbolic 3-manifold have? It is known, for example, that non-arithmetic two-bridge knot complements [32, Thm. 3.1] and link complements [24, Thm. 1.1] have no hidden symmetries. At the same time, there are a few examples and methods for constructing links admitting hidden symmetries; [9] gives one such construction. However, can we find examples of non-arithmetic hyperbolic 3-manifolds with the maximal number of hidden symmetries relative to volume? At most, the number of hidden symmetries of non-arithmetic hyperbolic 3-manifolds could grow linearly with volume; see the remark after Corollary 7.8. In Section 7, we construct examples exhibiting this optimal growth rate by considering particular half-twist partners of M_n , which we denote by M'_n ; see Figure 13. To the best of our knowledge, there are no other explicit families of non-arithmetic hyperbolic 3-manifolds realizing this growth rate described in the literature. It is interesting to see that among half-twist partners, which share a number of geometric and topological features, we can have as many and as few hidden symmetries as possible. This is highlighted in the following theorem.

Theorem 1.4. *For $n \geq 5$, each M_n has no hidden symmetries, while the half-twist partner M'_n has $2n$ hidden symmetries. Furthermore, the number of hidden symmetries of M'_n grows linearly with their volumes.*

Showing that each M'_n has $2n$ hidden symmetries first requires us to determine the symmetries of M'_n . This is a far more challenging task than determining the symmetries of M_n since quotienting by a visually obvious group of symmetries no longer gives a low volume orbifold. Instead, a careful analysis of how a certain cusp of M'_n can intersect totally geodesic surfaces in M'_n is used to limit the number of possible symmetries. From here, we can bootstrap off the fact that M_n and M'_n cover the same minimal orbifold \mathcal{O}_n and the degree of this covering map is the same in both cases since these manifolds have the same volume. Our analysis of symmetries and hidden symmetries of M_n determine exactly the degree of this cover. In turn, the degree of this cover and the number of symmetries of M'_n determine the number of hidden symmetries of M'_n .

This paper is organized into six additional sections beyond the introduction. In Section 2, we describe the geometric decomposition of pretzel FAL complements and their half-twist partners and provide an analysis of their cusp shapes. In Section 3, we show that a pretzel FAL complement is commensurable with any of its half-twist partners. In Section 4, we determine properties of the invariant trace fields of pretzel FAL complements; this work ultimately relies on the cusp shapes calculated earlier. Theorem 1.1 is proved in Section 5. In Section 6, we determine the symmetries of M_n , prove that M_n has no hidden symmetries, and prove Theorem 1.3. Finally, in Section 7, we analyze the symmetries and hidden symmetries of M'_n .

The authors acknowledge support from U.S. National Science Foundation grants DMS 1107452, 1107263, 1107367 "RNMS: Geometric Structures and Representation Varieties" (the GEAR Network). We would also like to thank Dave Futer for his helpful suggestions.

2. Geometric decomposition of fully augmented pretzel links

In this section, we first describe how to construct a pretzel FAL on the level of link diagrams in Section 2.1. We then describe how to build the complements of these links, both topologically and geometrically, in Section 2.2. Afterwards, we describe how to build a set of hyperbolic 3-manifolds that are both topologically and geometrically similar to a FAL complement in Section 2.3. Finally, in Section 2.4, we analyze the cusp shapes of pretzel FAL complements.

2.1. FAL diagrams. To construct a hyperbolic FAL, start with a diagram $D(K)$ of a link $K \subset \mathbb{S}^3$ that is *prime*, *twist reduced* with at least two twist regions, and *nonspittable*; see [14, Section 1] for appropriate definitions. We create a diagram for a FAL \mathcal{F} from $D(K)$ by first adding a crossing circle around each *twist region* in $D(K)$ (any maximal string of bigons arranged

end to end in the link diagram or a single crossing). After augmenting K by adding in the crossing circles, remove all full twists within each twist region. This leaves either no twists or a single half-twist in each twist region. The resulting link is our FAL \mathcal{F} , and Purcell [28, Theorem 2.5] shows that our assumptions on $D(K)$ imply that \mathcal{F} is hyperbolic. See the diagrams in Figure 1 for an example of a link diagram $D(K)$ and its corresponding FAL diagram $D(\mathcal{F})$.

A FAL decomposes into two sets of components: crossing circles (those added in the augmenting process) and knot circles (components coming from the original link K). We refer to a crossing circle as *twisted* if the two strands going through the crossing circle have a single half-twist. Otherwise, the two strands have no twists, and we refer to the corresponding crossing circle as *untwisted*.

For most of this paper, we will focus on FALs resulting from fully augmenting pretzel links. Let P_n denote a pretzel link with n twist regions, each with an even number of half-twists. We let \mathcal{P}_n denote the FAL resulting from fully augmenting P_n . Thus \mathcal{P}_n is a link with $2n$ components, half of which are (untwisted) crossing circles and the other half are knot circles. See Figure 2 for a diagram of \mathcal{P}_n .

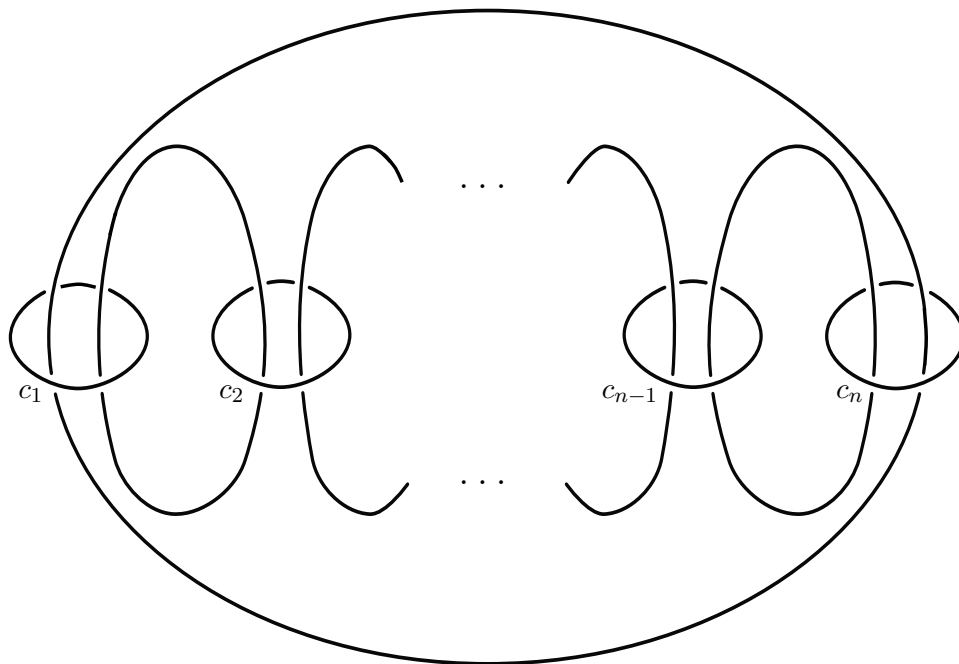


FIGURE 2. \mathcal{P}_n , with crossing circles labeled c_i , $i = 1, \dots, n$.

2.2. FAL complements. Given a hyperbolic FAL \mathcal{F} , consider the link complement $M_{\mathcal{F}} = \mathbb{S}^3 \setminus \mathcal{F}$. The following theorem collects a number of

geometric properties of FALs coming from [14] and [28]. In what follows, a *crossing disk* is a twice-punctured disk whose boundary is a crossing circle of a FAL.

Theorem 2.1. *Given a hyperbolic FAL \mathcal{F} , its complement $M_{\mathcal{F}}$ has the following properties:*

- (i) $M_{\mathcal{F}}$ decomposes into two identical ideal totally geodesic polyhedra, P_{\pm} , all of whose dihedral angles are right angles.
- (ii) The faces of these polyhedra can be checkerboard colored shaded and white, where shaded faces are all triangles coming from crossing disks and white faces are portions of the projection plane bounded by the knot circles.
- (iii) Intersecting a crossing disk with the projection plane creates two half disks. If we peel these two half disks apart, then four shaded faces are produced. Each of these four shaded faces is an ideal hyperbolic triangle, two in P_{+} and two in P_{-} .

Here, we give a short summary of how to explicitly build the polyhedra P_{\pm} and how to glue these polyhedra together to form a FAL complement. We will examine this decomposition in terms of our pretzel FAL complements, $M_n = \mathbb{S}^3 \setminus \mathcal{P}_n$, though this decomposition holds more generally for hyperbolic FALs. Examples where a FAL has some twisted crossing circles will be discussed in Section 2.3. For more explicit details on geometric decompositions of FALs, we refer the reader to [14] and [28]. By cutting $\mathbb{S}^3 \setminus \mathcal{P}_n$ along the projection plane, we subdivide our link complement into two identical 3-balls, one above the projection plane and one below. The crossing circles lie perpendicular to the projection plane, and so, each crossing disk is sliced in half by this process. To obtain our checkerboard coloring, peel each half crossing disk apart to obtain four shaded faces, two in each 3-ball. By shrinking the link components to become ideal vertices, we obtain the ideal polyhedra P_{\pm} , each with the desired checkerboard coloring, which is depicted in Figure 3. Note that, each crossing circle c_i from our link diagram produces two shaded triangular faces, c_i^a and c_i^b , in one of our polyhedra. In addition, there are $n + 2$ white faces, one for each region of the projection plane, which are labeled W_i , for $i = 1, \dots, n + 2$. To reverse this process, we first glue each white face in P_{+} to the white face in P_{-} that corresponds with the same white face in the projection plane. We then glue up pairs of shaded faces corresponding to the same half crossing disk in the same polyhedra.

The previous paragraph just gives a topological description of P_{\pm} . We now describe a geometric description of P_{\pm} as regular ideal polyhedra in \mathbb{H}^3 that are reflections of each other. The checkerboard coloring of the faces described in Theorem 2.1 actually provides instructions on how to explicitly build these two polyhedra in \mathbb{H}^3 . First, just consider the set of white faces. This set induces a circle packing of \mathbb{S}^2 , where we draw a circle for each

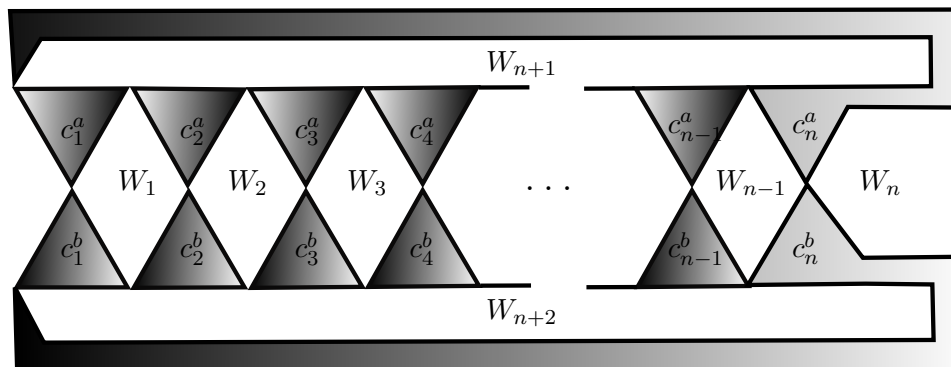


FIGURE 3. The checkerboard tiling of \mathbb{S}^2 associated to \mathcal{P}_n . This tiling determines the faces of the polyhedra P_{\pm} .

white face, and two circles are tangent to each other if the corresponding white faces share a vertex. The shaded triangular faces also induce a circle packing of \mathbb{S}^2 , dual to the white circle packing. The circle packing for the white faces is given in Figure 4. These circles are given the same labels as their corresponding faces in the checkerboard tiling of Figure 3. To build one of our polyhedra, extend these circles (both white and shaded) on $\mathbb{S}^2 \cong \partial\mathbb{H}^3$ to become totally geodesic planes in \mathbb{H}^3 . Cut away these planes to obtain P_+ . The polyhedron P_- can be obtained by reflecting P_+ across any of its white faces. Faces on P_{\pm} that are reflections of each other will be called *corresponding* faces.

This is a convenient time to introduce a helpful combinatorial structure related to the circle packing. It is used to provide examples of polyhedral partners for M_n in Subsection 2.3 and to prove that \mathcal{P}_n is commensurable with the reflection orbifold of P_+ . We proceed with the definition.

Definition 2.2. The *crushtacean* $C_{\mathcal{F}}$ of a FAL \mathcal{F} is the trivalent graph whose vertices correspond to shaded faces of the circle packing, and an edge is inserted between two vertices if and only if the corresponding shaded faces share a vertex in the circle packing.

The crushtacean was called the dual to the nerve of the circle packing by Purcell in [28]. It was first called the crushtacean in Chesebro–Deblois–Wilton [11] and named so because it can be constructed by crushing the shaded faces of the checkerboard tiling of \mathbb{S}^2 associated to \mathcal{P}_n down to vertices. This graph is trivalent since all shaded faces in this checkerboard tiling of \mathbb{S}^2 are triangles. In Figure 5, we show the crushtacean associated to our pretzel FAL \mathcal{P}_n , which comes from crushing the shaded faces seen in Figure 3 down to points.

2.3. Polyhedral Partners. In this section, we describe how to build sets of cusped hyperbolic 3-manifolds that have a number of geometric and topological features in common with a FAL complement. To start, fix a FAL \mathcal{F}

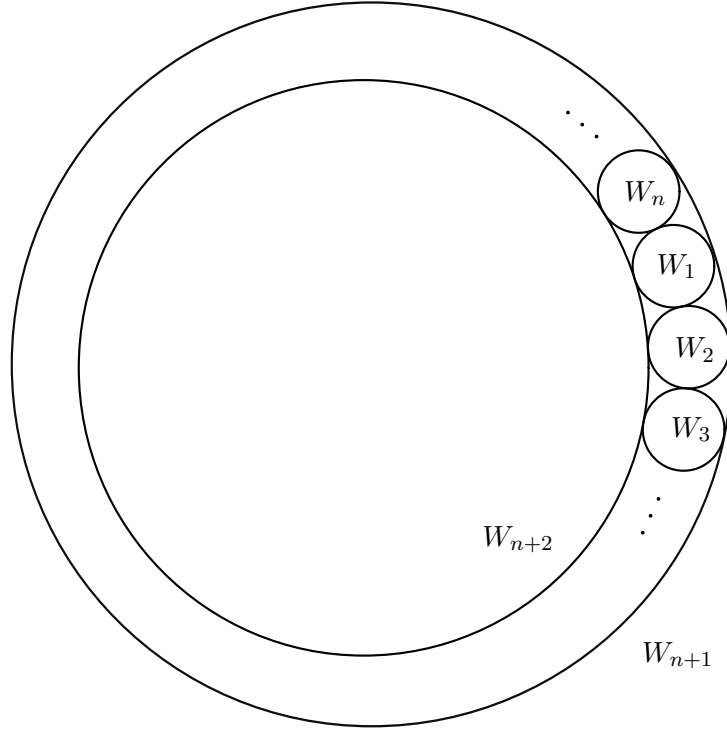


FIGURE 4. The circle packing of \mathbb{S}^2 for the white faces of the polyhedral decomposition of \mathcal{P}_n .

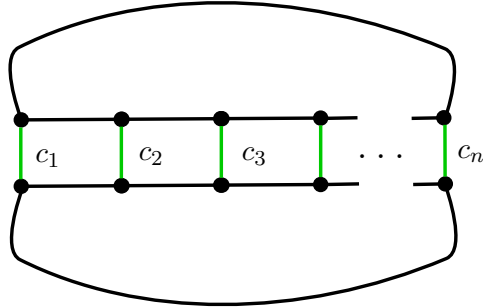


FIGURE 5. The crushtacean associated to the pretzel FAL \mathcal{P}_n . Edges coming from crossing circles have been labeled c_i for $i = 1, \dots, n$ and colored green.

that has n crossing circles. Each crossing circle is either twisted or untwisted. By varying which crossing circles contain a half-twist, we can create 2^n FAL link diagrams that all differ by some number of half-twists. Some of these diagrams could correspond to the same link. However, it is easy to show that many of these links (and their corresponding complements) will be different by considering the number of link components and their corresponding cusp

shapes. Nevertheless, all of these link complements are built from the same two identical ideal totally geodesic polyhedra, P_{\pm} , just with gluing instructions modified. Gluing shaded faces across their common vertex on the same polyhedron results in an untwisted crossing circle while gluing a shaded face in P_+ to its mate in P_- results in a twisted crossing circle (see [28, Figure 3]). Since this is the only modification made between two FALs that differ by some number of half-twists, we would expect this set of FAL complements to be “geometrically similar” to one another. This all motivates the following definitions.

Definition 2.3. Let \mathcal{F} be a hyperbolic FAL with n crossing circles, and fix an ordering on these crossing circles. At each crossing circle, assign a 0 to designate an untwisted crossing circle and assign a 1 to designate a twisted crossing circle. Define $\mathcal{F}' = \mathcal{F}(\epsilon_1, \epsilon_2, \dots, \epsilon_n)$ to be the hyperbolic FAL obtained from \mathcal{F} by assigning $\epsilon_i \in \{0, 1\}$ to the i^{th} crossing circle of \mathcal{F} . Any such $M_{\mathcal{F}'}$ is called a *half-twist partner* of $M_{\mathcal{F}}$. We let $HTP(\mathcal{F})$ designate the set of all half-twist partners of $M_{\mathcal{F}}$.

See the middle diagram of Figure 1 for a diagram of $\mathcal{P}_3(0, 1, 0)$.

In fact, we can generalize the above definition and just consider cusped hyperbolic 3-manifolds that are built from the polyhedra P_{\pm} with gluing instructions modified along shaded faces.

Definition 2.4. Let $M_{\mathcal{F}} = \mathbb{S}^3 \setminus \mathcal{F}$ be a hyperbolic FAL with associated polyhedra P_{\pm} . We say that M is a *polyhedral partner* of $M_{\mathcal{F}}$ if M can be constructed from P_{\pm} as follows:

- (i) Corresponding white faces of P_{\pm} are identified in the same manner as $M_{\mathcal{F}}$, and
- (ii) If $\varphi : G \rightarrow H$ identifies shaded faces G and H , then their corresponding faces are identified by conjugating φ with the reflection between P_{\pm} .

We let $PP(\mathcal{F})$ designate the set of all polyhedral partners of $M_{\mathcal{F}}$.

Remark. Polyhedral partners are precisely the manifolds obtained using the admissible gluing patterns defined by Harnois-Olson-Trapp in [15]. Theorem 1 and Lemma 1 of that paper combine to show that, assuming corresponding white faces are glued without twisting (criteria (i) of Definition 2.4), then criteria (ii) is necessary and sufficient to conclude that M is hyperbolic. Intuitively, polyhedral partners can be thought of as slicing $M_{\mathcal{F}}$ along the crossing disks, and then regluing in any manner that maintains a reflection surface.

The set $PP(\mathcal{F})$ is a rich collection of manifolds, some of which are topologically well understood. For convenience we include an example of a *nested link* which is a polyhedral partner of \mathcal{P}_5 ; for more detail see [15]. The combinatorial data that describes a nested link is an *edge-symmetric spanning forest* of the crushtacean. The left of Figure 6 shows an edge-symmetric

spanning forest of the crushtacean $\mathcal{C}_{\mathcal{P}_5}$. Note that each tree in the spanning forest admits an involution swapping the endpoints of the “middle” edge (hence the name edge-symmetric). The shaded faces whose corresponding vertices are swapped under this involution are glued together. The manifold resulting from this gluing is a *generalized* FAL complement in S^3 as seen on the right of Figure 6. Crossing circles of generalized FALs do not typically bound thrice punctured spheres. The links constructed as above are termed *nested* because the crossing circles nest in planes so that the regions between them form thrice punctured spheres. The point of this discussion is that $PP(\mathcal{F})$ is a much broader class of links than FALs, and many of them have explicit topological descriptions.

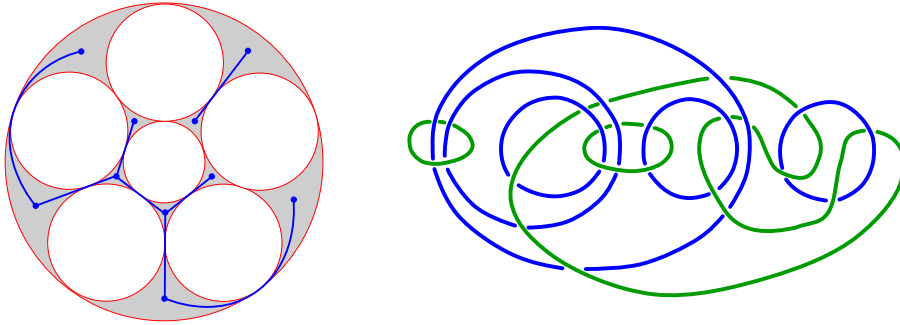


FIGURE 6. An edge-symmetric forest and corresponding polyhedral partner of \mathcal{P}_5

2.4. Cusp Analysis. In this section we compute the cusp shapes for the link complements M_n . The *cusp shape* of a cusp C of a cusped hyperbolic 3-manifold M is the Euclidean similarity class for the boundary torus ∂C , which can be computed as the ratio of the meridian over the longitude on ∂C . The calculations of this section will later assist in analyzing arithmeticity, invariant trace fields, and hidden symmetries of M_n .

Since there is a symmetry of M_n taking any component to any other, all cusp shapes are the same. We refer the reader to Figure 11 for a symmetric diagram of \mathcal{P}_n , where it is clear that each link component can be exchanged with its clockwise neighbor via a 90° rotation of the entire chain followed by a rotation. Symmetries of $(\mathbb{S}^3, \mathcal{P}_n)$ are also symmetries of M_n by Mostow–Prasad rigidity. Therefore, we isolate our attention to a single cusp corresponding to a crossing circle. In general, such a cusp has torus boundary tiled by two identical rectangles, coming from intersecting P_\pm with the horoballs centered at ideal vertices in $\partial\mathbb{H}^3$ corresponding to this crossing circle. For a more thorough and general description of cusp shapes for FALs, see Lemma 2.3 and Lemma 2.6 of [14].

Now recall that the circle packing for P_+ consists of a ring of n circles nested between concentric circles (see Figure 4). Assume that the ring of smaller circles are all unit circles, and consider the closer view given in Figure 7. The shape of the cusp corresponding to p will be determined.

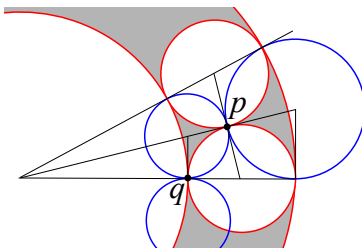


FIGURE 7. Partial circle packing of P_+

Inverting in a unit circle S centered at p sends p to infinity and the four faces of P_+ incident with p will invert to intersect a horosphere in a rectangle R , whose shape can be explicitly calculated. To do so, recall some elementary facts about inversion in planar circles.

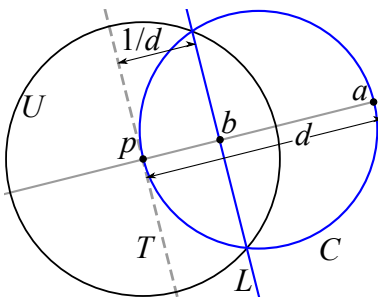


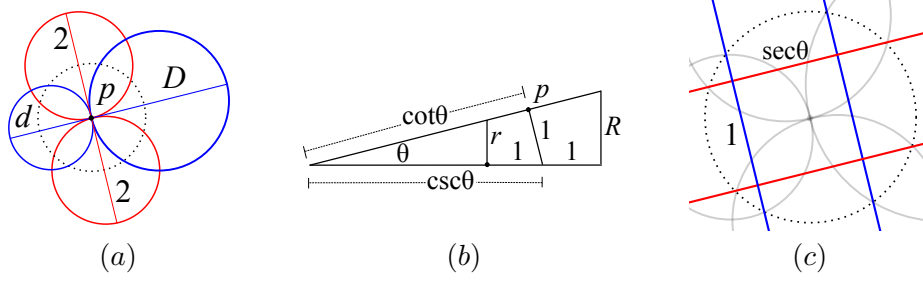
FIGURE 8. Inverting circles to lines

Let U denote a unit circle centered at p . Let C be any circle with diameter d through p , and with tangent line T there (see Figure 8). Inverting C across U yields a line L parallel to T . Moreover, the farthest point on C from p inverts to the closest point on L (the points labeled a and b in Figure 8). Since U is a unit circle, the distance from L to p is $1/d$.

We now return to the task of calculating the cusp shape for \mathcal{P}_n .

Lemma 2.5. *Let P_+ have p at infinity, and H be a horosphere centered at infinity. The shape of $R = P_+ \cap H$ is $i \sec(\pi/n)$.*

Proof. Starting with our original P_+ as in Figure 7, we let S be a unit sphere centered at p and invert in S . Focusing on those faces of P_+ incident

FIGURE 9. Inverting p to infinity

with p , we get the diagram in Figure 9(a) where the dotted circle is the boundary of S . The two unit circles (diameter 2) bound white faces of P_+ and invert to parallel lines one unit apart by the remarks preceding the lemma. The other circles bound shaded faces and invert to lines which are $\frac{1}{d} + \frac{1}{D}$ apart. We now calculate the diameters d and D .

To calculate the desired diameters, note that the centers of the unit circles are on a regular n -gon, and that the faint triangle in Figure 7 can be labeled as in Figure 9(b). Indeed, all the edges labeled 1 are radii of a unit circle in Figure 7. Letting $\theta = \pi/n$, trigonometry labels the sides of the right triangle with right angle at p . The edges labeled r and R are radii of the smaller and larger shaded circles (see Figure 7). Using similar triangles one computes that $r = \tan \theta (\csc \theta - 1)$ and $R = \tan \theta (\csc \theta + 1)$. The diameters are twice that, and one computes

$$\frac{1}{d} + \frac{1}{D} = \frac{1}{2 \tan \theta (\csc \theta - 1)} + \frac{1}{2 \tan \theta (\csc \theta + 1)} = \sec \theta.$$

Thus inversion in S sends p to infinity and P_+ intersects a horosphere in a rectangle with white sides 1 unit apart and shaded sides $\sec(\pi/n)$ apart (see Figure 9(c)).

□

Lemma 2.5 determines the shape of R near the cusp p . To get a fundamental rectangle, we need to include P_- near p . We state the result as the following proposition.

Proposition 2.6. *The cusp shape of each cusp of M_n is $2 \cos(\pi/n)i$.*

Proof. As mentioned earlier, there is a symmetry of M_n between any two components, so any two cusps will be isometric, for a particular choice of cusp expansion. This implies that all cusp shapes are isometric. Thus we calculate the shape of the cusp p . In Lemma 2.5 we showed that P_+ near p is a rectangle R with shaded sides length 1 and white sides length $\sec \theta$. Since p is a crossing circle cusp, the shaded sides of R are identified, while the white are not. To get a fundamental region for the cusp we note that P_- is the reflection of P_+ across any white side. Thus a fundamental region is two

tiles identical to that of Lemma 2.5 glued along an white face, resulting in a 2-by-sec θ rectangle. Rescaling to have unit meridian gives Figure 10(a). \square

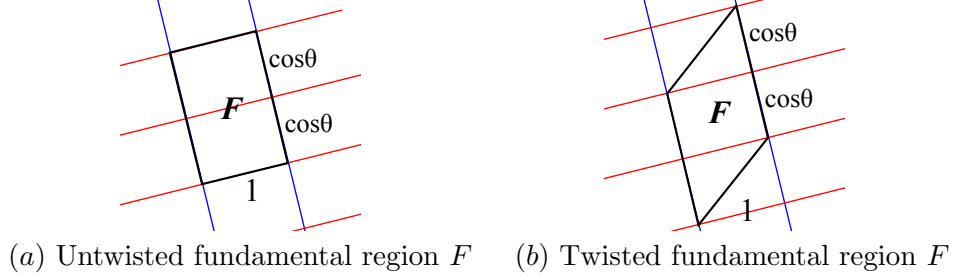


FIGURE 10. Untwisted and twisted cusp shapes

Remark: We point out that since p is a crossing circle, the meridian lies in the reflection surface and on the white sides of the fundamental region (labeled sec θ in Figure 9(c)). The longitude lies in the shaded faces. If one normalizes the meridian to length 1, the corresponding longitude has length $2 \cos(\pi/n)$.

Before moving on, we pause to consider the cusp shape of a half-twist partner of M_n . The shape itself depends on whether the half-twist is positive or negative, but as the resulting manifolds are homeomorphic (they differ by a full-twist on the corresponding crossing disk) the distinction does not affect the invariants under consideration.

Lemma 2.7. *Let C be a twisted crossing circle cusp in a half-twisted partner of M_n . The cusp shape of C is $\frac{2 \cos(\pi/n)i}{1 \pm \cos(\pi/n)i}$.*

Proof. Changing from an untwisted to a twisted crossing circle alters the gluing pattern on the shaded faces. For untwisted crossing circles, as in Proposition 2.6, shaded faces are glued straight across, while for twisted crossing circles the gluing map shifts a single tile in the shaded direction (see [14, Figure 7]). Thus, scaling so that the distance between shaded faces is one, a fundamental parallelogram has longitude $2 \cos(\pi/n)i$ and meridian $1 \pm \cos(\pi/n)i$ (see Figure 10(b) for the $1 + \cos(\pi/n)i$ case). The result follows. \square

3. Hyperbolic reflection orbifolds

In this section, we establish a strong commensurability relation for our pretzel FAL complements - we show that any M_n , along with all of its half-twist partners, is commensurable with the *hyperbolic reflection orbifold* associated with P (a single copy of P_{\pm}). This is the orbifold $\mathcal{O}_P = \mathbb{H}^3/\Gamma_P$,

where Γ_P is generated by reflections in the faces of P . This commensurability relation will be used to help determine arithmeticity and hidden symmetries of half-twist partners in Section 5 and Section 7, respectively.

While it perhaps seems probable that any FAL complement will be commensurable with its associated hyperbolic reflection orbifold, this is not always the case. For instance, Chesebro–DeBlois–Wilton in Section 7.2 of [11] describe an infinite family of FALs that are not commensurable with any hyperbolic reflection orbifold. Fortunately, in the same paper, a criterion is established to guarantee that FAL complements with a certain combinatorial symmetry will be commensurable with their associated hyperbolic reflection orbifolds. This criterion is stated in terms of the crushtacean of Definition 2.2. The following lemma is a rewording of [11, Lemma 7.4]; the commensurability conclusion stated in our version is noted in the paragraph following the proof of Lemma 7.4 in [11].

Lemma 3.1. [11, Lemma 7.4] *Let \mathcal{F} be a FAL with crushtacean $C_{\mathcal{F}}$. Suppose $C_{\mathcal{F}}$ has the property that for each crossing circle component c_i of \mathcal{F} , corresponding to an edge e_i of $C_{\mathcal{F}}$ with vertices v_i and v'_i ,*

- (i) *if c_i is untwisted, then there is a reflective involution of $C_{\mathcal{F}}$ preserving e_i and exchanging v_i and v'_i .*
- (ii) *if c_i is twisted, then there is a rotational involution of $C_{\mathcal{F}}$ preserving e_i and exchanging v_i and v'_i .*

Then $M_{\mathcal{F}}$ is commensurable with its associated reflection orbifold.

Proposition 3.2. *Suppose $M \in \text{HTP}(\mathcal{P}_n)$. Then M is commensurable with the reflection orbifold associated to M_n . In particular, if $M, M' \in \text{HTP}(\mathcal{P}_n)$, then M and M' are commensurable.*

Proof. The crushtacean for P_n is given in Figure 5, where all of the edges coming from crossing circles are labeled c_1, \dots, c_n . Note that, any half-twist partner of P_n also has the same crushtacean with the same edge colorings. Consider the horizontal line intersecting all of the green edges of our crushtacean in their respective midpoints. Both reflecting across this line and rotating 180° across this line provide involutions of our crushtacean that preserve any crossing circle edge e_i while exchanging its respective vertices. Thus, any $M \in \text{HTP}(\mathcal{P}_n)$ satisfies the criteria of Lemma 3.1, and so, is commensurable with the reflection orbifold associated to M_n . The second statement follows from the fact that commensurability is an equivalence relation. \square

4. Cusp and trace fields

The goal of this section is to prove Theorem 1.2, which is a key component for the proof of Theorem 1.1. A complete hyperbolic 3-manifold M of finite volume can be identified with the quotient \mathbb{H}^3/Γ where $\Gamma \subset \text{PSL}_2(\mathbb{C})$ is a lattice. The *trace field* of M , denoted $\mathbb{Q}(\text{tr } \Gamma)$, is the field generated by the

traces of the elements of Γ . Similarly, the *invariant trace field* of M , denoted kM , is the field generated by the traces of the products of squares of the elements of Γ . When M is cusped, its *cuspidal field*, denoted cM , is the field generated by the cusp shapes of M . These fields are finite extensions of \mathbb{Q} and satisfy the inclusions $cM \subset kM \subset \mathbb{Q}(\text{tr } \Gamma)$ [26]. In general, these fields are distinct, however in the case of FALs, by [12, Theorem 6.1.6] and [20, Cor. 4.2.2], these fields coincide, i.e. $cM = kM = \mathbb{Q}(\text{tr } \Gamma)$. This enables us to determine the invariant trace field of each M_n and its half-twist partners.

Proposition 4.1. *If $M \in \text{HTP}(\mathcal{P}_n)$, $n \geq 3$, then $kM = \mathbb{Q}(\cos(\pi/n)i)$.*

Proof. By Proposition 2.6, the cusp shapes of M_n are all $2\cos(\pi/n)i$, and hence, $cM_n = \mathbb{Q}(\cos(\pi/n)i)$. Flint [12, Theorem 6.1.6] shows $cM_n = kM_n$. Since the invariant trace field is a commensurability invariant and half-twist partners are commensurable by Proposition 3.2, it follows that $kM = \mathbb{Q}(\cos(\pi/n)i)$. \square

Based on Proposition 4.1, it's natural to ask if this result extends to polyhedral partners that are not half-twist partners. While half-twist partners always share the same invariant trace field (both by Flint's work [12] and Theorem 5.6.1 from [20]), it does not seem immediately obvious that the techniques used in these papers would extend to polyhedral partners. This all motivates the following question.

Question 4.2. *How much can cusp and trace fields vary among polyhedral partners who are not half-twist partners?*

Even though we have identified distinct primitive elements, $\cos(\pi/n)i$, in each kM_n , the fields they generate may be isomorphic. To differentiate them, we compute the degree of the field extension $[kM_n : \mathbb{Q}]$.

Lemma 4.3. *For each $n \geq 3$, $[kM_n : \mathbb{Q}] = \phi(n)$, the Euler totient function.*

Proof. Since $(\cos(\pi/n)i)^2 = -\cos^2(\pi/n) = -\frac{1}{2}(\cos(2\pi/n) + 1)$, kM_n is a quadratic extension of $\mathbb{Q}(\cos(2\pi/n))$. Lehmer showed that $[\mathbb{Q}(\cos(2\pi/n)) : \mathbb{Q}] = \phi(n)/2$ [19] [36]. The result follows. \square

In the proof of Lemma 4.3, we see that for each $n \geq 3$, kM_n is an imaginary quadratic extension of its totally real subfield $\mathbb{Q}(\cos(2\pi/n))$, or in other words, is a CM-field. In particular, kM_n has no real places (cf. [7, Thm. A]).

Lemma 4.4. *For any $d \in \mathbb{N}$, there exists an $n_d \in \mathbb{N}$ such that for all $n \geq n_d$, $[kM_n : \mathbb{Q}] \geq d$.*

Proof. This follows from the fact that $\phi(n)$ can be bounded from below by an increasing, unbounded function. For example, it is known that for $n \geq 3$, $\phi(n) > \frac{n}{e^\gamma \log \log n + \frac{3}{\log \log n}}$, where γ is Euler's constant [2, Theorem 8.8.7]. \square

Putting these lemmas together, we get the following finiteness result.

Proposition 4.5. *For each $n \geq 3$, there are only finitely many n_i such that $kM_{n_i} \cong kM_n$.*

Proof. Suppose that for some $m \geq 3$, $kM_m \cong kM_n$. Then $[kM_m : \mathbb{Q}] = [kM_n : \mathbb{Q}]$ and by Lemma 4.4, there are only finitely many m for which this can hold. \square

These results, taken together, now prove Theorem 1.2. Meanwhile, Proposition 4.5 motivates the following question:

Question 4.6. *Does $m \neq n$ imply that $kM_m \not\cong kM_n$?*

If $kM_m \cong kM_n$, then it is necessarily the case that $\phi(m) = \phi(n)$. Since for a fixed $d \in \mathbb{N}$, $\phi(x) = d$ has only finitely many solutions, one strategy is to fix d and then compare the fields kM_n for each $n \in \phi^{-1}(d)$. In the low degree cases, direct computations are possible and the answer to Question 4.6 is yes. For example, $\phi(n) = 2$ only when n is 3, 4, or 6. A direct computation here shows that $kM_3 = \mathbb{Q}(\sqrt{-1})$, $kM_4 = \mathbb{Q}(\sqrt{-2})$, and $kM_6 = \mathbb{Q}(\sqrt{-3})$. More generally, implementing SAGE code, we are able to compute kM_n for each $n \leq 150$, and by comparing degrees and discriminants, verify that each are distinct.

Proposition 4.7. *If $m, n \in \{3, 4, \dots, 150\}$ and $m \neq n$, then $kM_m \not\cong kM_n$.*

Unfortunately, the problem of understanding the solutions to $\phi(x) = d$ for large d becomes quite complicated (see, for example, [13]) which suggests that one should look for another strategy. Should the answer to Question 4.6 be yes, then this would supply an alternative proof to Corollary 6.4, below.

5. Arithmeticity

In this section, we completely classify which pretzel FAL complements (along with their half-twist partners) are arithmetic. In order to do this, we employ two arguments: one argument uses short geodesics to rule out arithmeticity for most pretzel FAL complements and the other argument uses our invariant trace field calculations from Section 4 to take care of the remaining cases.

There are very strong restrictions placed on the possible lengths of short geodesics in a cusped arithmetic hyperbolic 3-manifold, especially arithmetic link complements. Essentially, such manifolds rarely have short geodesics, and if they do, only a specific set of short lengths can be realized. This is highlighted in the following work from Neumann and Reid:

Theorem 5.1. [26, Corollary 4.5, Theorem 4.6, Corollary 4.7] *Let $M = \mathbb{H}^3/\Gamma$ be a hyperbolic link complement. If M is arithmetic and contains a geodesic of length less than $1.9248473002\dots$, then Γ is commensurable with*

PSL_2O_d with $d \in \{1, 2, 3, 7, 11, 15, 19\}$ and the length of any such geodesic is one of the values from Table 1 (page 283 of [26]). If M contains a geodesic of length less than 0.862554627, then M must be non-arithmetic.

Here, we will use Theorem 5.1 to show that most $M_n = \mathbb{S}^3 \setminus \mathcal{P}_n$ (and their respective polyhedral partners) are non-arithmetic.

Proposition 5.2. *If $n \geq 7$, then M_n and all of its polyhedral partners are non-arithmetic.*

Proof. We first show that M_n has a sufficiently short geodesic when $n \geq 7$ and then apply Theorem 5.1 to rule out arithmeticity. The fact that polyhedral partners are also non-arithmetic will immediately follow from how this geodesic is constructed.

Consider the circle packing used to build the polyhedra P_+ for M_n shown in Figure 4. The circles W_{n+1} and W_{n+2} bound planes that contain faces of P_+ . Let γ^+ be the vertical line segment through the origin that is the common perpendicular from W_{n+1} to W_{n+2} . The radii of the W_i are needed to compute the length of γ^+ , and Figures 7 and 9(b) show that they can be chosen to be $\csc(\pi/n) \pm 1$. The hyperbolic length of γ^+ is therefore $\ell(\gamma^+) = \ln \left(\frac{\csc(\pi/n)+1}{\csc(\pi/n)-1} \right)$.

To construct the short geodesic γ , let P_- be the reflection of P_+ across the plane H whose boundary is W_{n+2} and let γ^- be the reflection of γ^+ . The polyhedron $P_+ \cup P_-$ is a fundamental region for M_n , with the innermost face (bounded by W_{n+1}) glued to the outermost (the reflection of the innermost across H) by a dilation. Thus the curve $\gamma^+ \cup \gamma^-$ projects to a closed geodesic γ in M_n . Since the curves γ^\pm are isometric, the length of γ in M_n is twice that of γ^+ , or $\ell(\gamma) = 2 \ln \left(\frac{\csc(\pi/n)+1}{\csc(\pi/n)-1} \right)$.

For $n \geq 15$, this creates a geodesic of length less than 0.862554627, and so, by Theorem 5.1, any such M_n is non-arithmetic. At the same time, for $7 \leq n \leq 15$, we can compare $\ell(\gamma)$ to the geodesic lengths given in Table 1 on page 283 in the original statement of Theorem 5.1 in [26]. Since $\ell(\gamma)$ does not match up with any of these values, we now know that M_n is non-arithmetic for $n \geq 7$.

Finally, we note that the geodesic segments γ^+ and γ^- run between white faces in their respective polyhedra, and never intersect the shaded faces. Thus, their union will always project to a geodesic of length $\ell(\gamma)$ in any polyhedral partner of M_n . Therefore, the same short geodesic analysis applied in the previous paragraph also applies to any polyhedral partner of M_n , as needed. \square

Proposition 5.2 applies to M_n and all of its polyhedral partners, making it applicable to a broad class of hyperbolic manifolds (see Remark 2.3). We now focus on the manifolds M_n (and their half-twist partners), and classify which are arithmetic. To do so, both Proposition 5.2 and our invariant trace field calculations limit the possible values of n to 3, 4, 6, and we use

Vinberg's criteria to show M_6 is not arithmetic. These techniques are more limited in scope, and do not immediately apply to polyhedral partners of M_n .

Theorem 1.1. *M_n and all of its half-twist partners are arithmetic if and only if $n = 3, 4$.*

Proof. For a cusped, finite volume, hyperbolic manifold to be arithmetic, it is a necessary condition that its invariant trace field be an imaginary quadratic extension of \mathbb{Q} [20, Theorem 8.2.3]. By Proposition 4.1, the invariant trace field of M_n is $kM_n = \mathbb{Q}(\cos(\pi/n)i)$, which by Lemma 4.3, has degree $[kM_n : \mathbb{Q}] = \phi(n)$. A straight forward computation shows that $\phi(n) = 2$ implies that n is 3, 4, or 6. Thus only M_3 , M_4 and M_6 can be arithmetic. Additionally, Proposition 5.2 also implies that only M_n with $n \leq 6$ could be arithmetic.

The fact that M_3 and M_4 are arithmetic was observed by Thurston in [33, Chapter 6], a fact that also follows from [11, Lemma 7.6 and Corollary 7.5] where they show that the crusstaceans of M_3 and M_4 imply they are arithmetic.

We now analyze the case of M_6 . Let P denote the hyperbolic polyhedra associated to M_6 . By Proposition 3.2, M_6 is commensurable to the hyperbolic orbifold $\mathcal{O} = \mathbb{H}^3/\Gamma_P$ generated by reflections through the faces of P . Since arithmeticity is a commensurability invariant, it suffices to analyze \mathcal{O} . Associated to P is the Gram matrix $G(P)$, which encodes the angles between intersecting faces, and distances between disjoint faces of P . Vinberg's arithmeticity criterion in this context states that for \mathcal{O} to be arithmetic, it is necessary that each entry in the Gram matrix is an algebraic integer [20, 10.4.5]. A direct calculation shows this fails for the polyhedron P , which we now describe.

The Gram matrix entry corresponding to disjoint faces is $-2 \cosh(\ell(\gamma))$ where $\ell(\gamma)$ is the length of the common perpendicular between the faces. Let γ^- be the common perpendicular between faces W_{n+1} and W_{n+2} of Figure 4. When $n = 6$ the calculations of the proof of Proposition 5.2 reduce to $\ell(\gamma^-) = \ln\left(\frac{\csc(\pi/6)+1}{\csc(\pi/6)-1}\right) = \ln 3$, and the corresponding Gram matrix entry is $-2 \cosh(\ln 3) = -10/3$. Hence Vinberg's criterion fails, and M_6 is not arithmetic.

The extension to half-twist partners follows from Proposition 3.2. \square

Remark 5.3. The manifold M_6 is a rather intriguing example. We know $kM_6 = \mathbb{Q}(\sqrt{-3})$. In [33, Chapter 6], Thurston remarked that the volume of M_6 is 20 times the volume of the figure-eight knot complement, the arithmetic knot complement whose invariant trace field happens to be $\mathbb{Q}(\sqrt{-3})$. Despite these coincidences, M_6 is not arithmetic. This suggests that M_6 should be considered in the future when looking for non-arithmetic manifolds that share other attributes with arithmetic manifolds.

6. Symmetries and hidden symmetries

Here, we completely classify the symmetries and hidden symmetries of pretzel FAL complements. As a corollary, we are able to completely determine when pretzel FAL complements (and their half-twist partners) are commensurable with one another. First, we define these terms and introduce some important tools necessary to understand why symmetries and hidden symmetries play a pivotal role in analyzing commensurability classes of hyperbolic 3-manifolds.

Given a hyperbolic 3-manifold $M = \mathbb{H}^3/\Gamma$, the group of symmetries of M , denoted $Sym(M)$, is the group of self-homeomorphisms of M , up to isotopy. This group is homeomorphic to $N(\Gamma)/\Gamma$, where $N(\Gamma)$ denotes the normalizer of Γ in $Isom(\mathbb{H}^3)$. Let $Sym^+(M) \cong N^+(\Gamma)/\Gamma$ denote the subgroup of orientation-preserving symmetries, where $N^+(\Gamma)$ denotes the restriction of $N(\Gamma)$ to orientation-preserving isometries. To define a hidden symmetry of M , we first need to introduce the *commensurator* of Γ , which is $C(\Gamma) = \{g \in Isom(\mathbb{H}^3) : |\Gamma : \Gamma \cap g\Gamma g^{-1}| < \infty\}$. We let $C^+(\Gamma)$ denote the restriction of $C(\Gamma)$ to orientation-preserving isometries of \mathbb{H}^3 .

Studying commensurators of Γ is another way to approach studying the commensurability class of M : M is commensurable with another hyperbolic 3-manifold N if and only if the corresponding commensurators of M and N are conjugate in $Isom(\mathbb{H}^3)$; see Lemma 2.3 of [35]. Note that, $\Gamma \subset N(\Gamma) \subset C(\Gamma)$. *Hidden symmetries* of M correspond with nontrivial elements of $C(\Gamma)/N(\Gamma)$. Geometrically, M admits a hidden symmetry if there exists a symmetry of a finite cover of M that is not a lift of an isometry of M . See [35] for more background on hidden symmetries and commensurators of hyperbolic 3-manifolds.

Hidden symmetries also play a defining role in the arithmeticity of hyperbolic 3-manifolds, and more generally, hyperbolic 3-orbifolds. The work of Margulis [21] shows that $C(\Gamma)$ is discrete in $Isom(\mathbb{H}^3)$ with Γ finite index in $C(\Gamma)$ if and only if Γ is non-arithmetic. Thus, $M = \mathbb{H}^3/\Gamma$ is arithmetic if and only if M has infinitely many hidden symmetries. Furthermore, in the non-arithmetic case, the hyperbolic 3-orbifold $\mathcal{O} = \mathbb{H}^3/C(\Gamma)$ is the unique minimal orbifold in the commensurability class of M . This minimal orbifold (and its orientable variant: $\mathcal{O}^+ = \mathbb{H}^3/C^+(\Gamma)$) will play an essential role in examining commensurability classes here. In particular, if M admits no hidden symmetries, then $\mathcal{O} = \mathbb{H}^3/N(\Gamma) = M/Sym(M)$. In this case, we only need to determine the symmetries of M to get our hands on the minimal orbifold in the commensurability class of M .

Now, we focus on determining the symmetries and hidden symmetries of our pretzel FAL complements. For our purposes, we will work with a symmetric diagram of \mathcal{P}_n ; see Figure 11. These links and their symmetric diagrams were examined in Example 6.8.7 of Chapter 6 of Thurston's notes [33]. In this setting, Thurston used D_{2n} to denote our \mathcal{P}_n .

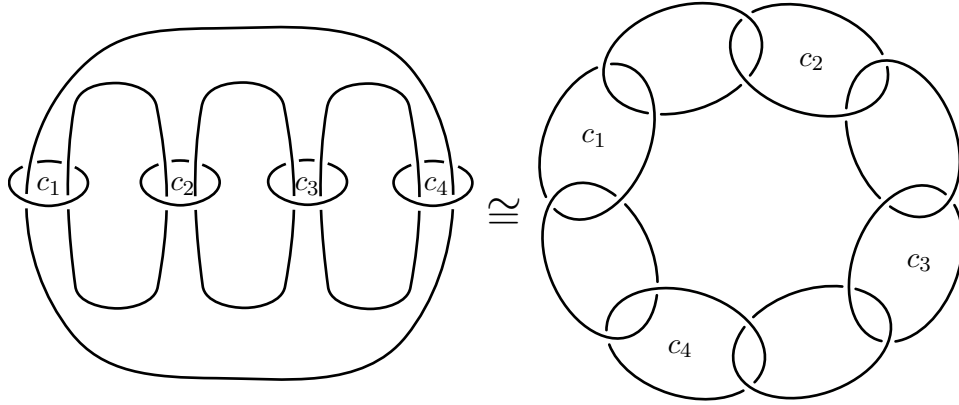
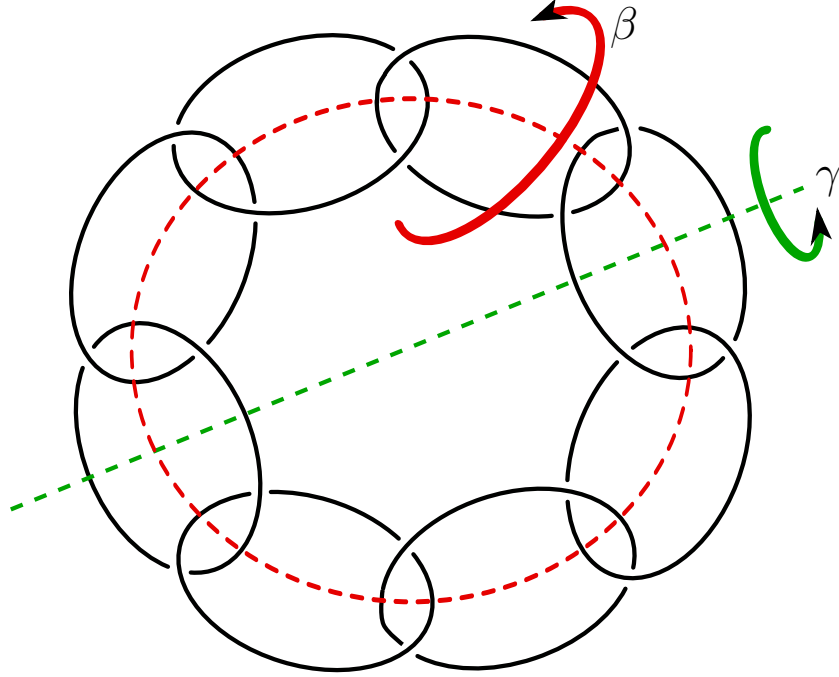


FIGURE 11. Two diagrams of the same pretzel FAL, \mathcal{P}_4 . The left diagram comes from augmenting a pretzel link and the right diagram is the symmetric diagram as described in Thurston's notes. Crossing circles are labeled in each diagram.

In what follows, for a link $K \subset \mathbb{S}^3$, we let $Sym(\mathbb{S}^3, K)$ denote the group of homeomorphisms of the pair (\mathbb{S}^3, K) , up to isotopy. We use $Sym^+(\mathbb{S}^3, K)$ to denote the restriction to orientation-preserving symmetries. First, we identify a visually obvious subgroup of $Sym^+(\mathbb{S}^3, \mathcal{P}_n)$, as viewed from the symmetric diagram of \mathcal{P}_n . Let α be the symmetry that takes every link component to its (clockwise) neighbor, swapping each knot component with a crossing circle component. Let β be the 180° rotation about the circular axis depicted in Figure 12. Let γ be the 180° rotation about the linear axis depicted in Figure 12. These three elements generate a group of orientation-preserving symmetries of order $8n$, which we denote by G_n^+ .

Note that, $G_n^+ \leq Sym^+(\mathbb{S}^3, \mathcal{P}_n) \leq Sym^+(M_n)$, and both of these containments could be strict. By Mostow–Prasad Rigidity, the group of symmetries of a hyperbolic link in \mathbb{S}^3 is a subgroup of the symmetries of the corresponding link complement. For hyperbolic knots, these two groups are always equal by the work of Gordon–Luecke. However, for hyperbolic links with more than one component, this could be a strict containment; see [16] for such an example. At the same time, it is also possible that \mathcal{P}_n has orientation-preserving symmetries beyond the ones we identified from its symmetric diagram. Our first goal is to show that we have identified all orientation-preserving symmetries, and in fact, all the hidden symmetries of M_n .

Theorem 6.1. *For any non-arithmetic $M_n = \mathbb{S}^3 \setminus \mathcal{P}_n$, we have that $G_n^+ = Sym^+(M_n)$ and M_n admits no (orientation-preserving) hidden symmetries.*


 FIGURE 12. A symmetric diagram for \mathcal{P}_4

To prove this theorem, we first need a lemma about the volumes of M_n . Let $\mathcal{L}(\theta) = -\int_0^\theta \ln |2 \sin(x)| dx$ denote the Lobachevsky function. In Example 6.8.7 in Chapter 6 of Thurston's notes [33], the following volume formula is given: $\text{vol}(M_n) = 8n(\mathcal{L}(\frac{\pi}{4} + \frac{\pi}{2n}) + \mathcal{L}(\frac{\pi}{4} - \frac{\pi}{2n}))$. Let $f(n) = \frac{\text{vol}(M_n)}{8n}$. This function will actually give us the volume of the minimal orbifold in the commensurability class of M_n .

Let v_{oct} denote the volume of a regular ideal hyperbolic octahedron.

Lemma 6.2. *The function $f(n)$ is strictly increasing and $\lim_{n \rightarrow \infty} f(n) = \frac{v_{\text{oct}}}{4} \approx 0.915965$, for $n > 2$.*

Proof. A great exercise for your calculus students shows that $f'(n) = \frac{\pi}{2n^2} \ln \left| \frac{\sin(\frac{\pi}{4} + \frac{\pi}{2n})}{\sin(\frac{\pi}{4} - \frac{\pi}{2n})} \right|$. Notice that $f'(n) > 0$ if and only if $\frac{\sin(\frac{\pi}{4} + \frac{\pi}{2n})}{\sin(\frac{\pi}{4} - \frac{\pi}{2n})} > 1$. This second inequality holds if and only if $\sin(\frac{\pi}{4} + \frac{\pi}{2n}) > \sin(\frac{\pi}{4} - \frac{\pi}{2n})$. This inequality holds for $n > 2$ since $\sin(\theta)$ is increasing on the interval $0 < \theta < \frac{\pi}{2}$. Thus, since $f'(n) > 0$ on our domain, we can conclude that $f(x)$ is strictly increasing on our domain.

Also, we have that $\lim_{n \rightarrow \infty} f(n) = \lim_{n \rightarrow \infty} (\mathcal{L}(\frac{\pi}{4} + \frac{\pi}{2n}) + \mathcal{L}(\frac{\pi}{4} - \frac{\pi}{2n})) = 2\mathcal{L}(\frac{\pi}{4}) = \frac{v_{\text{oct}}}{4}$. \square

Now, we prove Theorem 6.1. In this proof, any symmetries or hidden symmetries will be assumed to be orientation-preserving. In what follows, a hyperbolic 3-orbifold has a *rigid cusp* if it has a cusp whose cross section

is of the form $\mathbb{S}^2(2, 4, 4)$, $\mathbb{S}^2(3, 3, 3)$, or $\mathbb{S}^2(2, 3, 6)$. Likewise, a cusp of a hyperbolic 3-orbifold is called a *non-rigid cusp* if a cross section of this cusp is topologically either a torus or $\mathbb{S}^2(2, 2, 2, 2)$.

Proof of Theorem 6.1. By Margulis's Theorem, we know that for any non-arithmetic M_n , there exists a unique minimal (orientation-preserving) orbifold in its commensurability class, namely $\mathcal{O}_n^+ = \mathbb{H}^3/C^+(\Gamma_n)$. Let $Q_n^+ = M_n/G_n^+$. If M_n has any hidden symmetries or any symmetries beyond the ones contained in G_n^+ , then $Q_n^+ \neq \mathcal{O}_n^+$, and in particular, Q_n^+ is a non-trivial cover of \mathcal{O}_n^+ . Since $|G_n^+| = 8n$, we have that $\text{vol}(Q_n^+) = \frac{\text{Vol}(M_n)}{8n} = f(n)$. Lemma 6.2 implies that $\text{vol}(Q_n^+) < 0.915965$ for all non-arithmetic M_n . Since we are assuming Q_n^+ non-trivially covers \mathcal{O}_n^+ , we have that $\text{vol}(\mathcal{O}_n^+) \leq \frac{\text{vol}(Q_n^+)}{2} < 0.4579825$. We now consider two cases based on the cusp of Q_n^+ . Note that, since G_n^+ contains a subgroup of symmetries exchanging all of the link components, the orbifold Q_n^+ only has one cusp.

Case 1: Suppose the cusp of Q_n^+ is non-rigid. In this case, our volume bound guarantees that \mathcal{O}_n^+ is on the list of smallest volume (orientable) hyperbolic 3-orbifolds with a non-rigid cusp highlighted in the work of Adams; see Corollary 4.2 and Lemma 7.1 of [1]. In particular, all of these orbifolds are arithmetic. But M_n is non-arithmetic and since arithmeticity is a commensurability invariant, this would imply that \mathcal{O}_n^+ is non-arithmetic, giving a contradiction.

Case 2: Suppose the cusp of Q_n^+ is rigid. In this case, the cusp field of Q_n^+ must be contained in $\mathbb{Q}(i)$ or $\mathbb{Q}(\sqrt{-3})$. The proof of Theorem 1.1 shows that the invariant trace field of a non-arithmetic M_n (which is the same as the cusp field of M_n) could be $\mathbb{Q}(i)$ or $\mathbb{Q}(\sqrt{-3})$ only if $n = 6$. From here, we determine $\text{Sym}^+(M_6)$ via SnapPy and see that it has order 48 (SnapPy actually determines the full symmetry group, which is order 96). Since $|G_6| = 48$, we can conclude that G_6 contains all orientation-preserving symmetries of M_6 . Now, suppose M_6 admits hidden symmetries. Then we have a non-normal cover of \mathcal{O}_6^+ by Q_6^+ . Thus, $\text{vol}(\mathcal{O}_6^+) \leq \frac{\text{vol}(Q_6^+)}{3} = f(6)/3 \approx 0.281928224$. However, this is impossible since this is smaller than the smallest volume for an orientable, one-cusped hyperbolic 3-orbifold; see [22]. Thus, M_6 admits no hidden symmetries.

In conclusion, we must have that $Q_n^+ = \mathcal{O}_n^+$, which implies that M_n has no hidden symmetries and $G_n^+ = \text{Sym}^+(M_n)$. \square

There are a number of useful applications of Theorem 6.1. First off, we can extend this same line of argument to determine $\text{Sym}(M_n)$ and show that M_n also admits no orientation-reversing hidden symmetries. Every \mathcal{P}_n admits an orientation-reversing symmetry σ given by reflection in the projection plane, and so, by Mostow–Prasad Rigidity, induces an orientation-reversing symmetry for M_n , which we shall also denote by σ . Let G_n be the group generated by the elements of G_n^+ and σ . This group has order $16n$.

Corollary 6.3. *For any non-arithmetic $M_n = \mathbb{S}^3 \setminus \mathcal{P}_n$, we have that $G_n = \text{Sym}(M_n)$ and M_n admits no hidden symmetries (both orientation-preserving and reversing).*

Proof. Consider the quotient $Q_n = M_n/G_n$. If we suppose Q_n is not the minimal orbifold in its respective commensurability class, then we can now apply the same argument used in the proof of Theorem 6.1. \square

Another nice application is the fact that we can now determine which pretzel FAL complements are commensurable with each other. The corollary given below describes this commensurability relation, and also, confirms Conjecture 6.2.6 from the work of Flint [12].

Corollary 6.4. *Suppose $M \in \text{HTP}(\mathcal{P}_m)$ and $N \in \text{HTP}(\mathcal{P}_n)$. Then M and N are commensurable if and only if $m = n$.*

Proof. First off, Proposition 3.2 implies that if $m = n$, then M and N are commensurable. For the other direction, we break this proof down into a few cases, depending on whether or not M_n and M_m are arithmetic.

Case 1: Suppose M_n and M_m are non-arithmetic. By Margulis, there exists a unique minimal (orientable) hyperbolic 3-orbifold $\mathcal{O}_n^+ = \mathbb{H}^3/C^+(\Gamma_n)$ in the commensurability classes of $M_n = \mathbb{H}^3/\Gamma_n$. Likewise, we have that $\mathcal{O}_m^+ = \mathbb{H}^3/C^+(\Gamma_m)$ is the minimal orbifold for M_m . By Theorem 6.1, we know that \mathcal{O}_n^+ is just the quotient M_n/G_n^+ , where $|G_n^+| = 8n$. Thus, $\text{vol}(\mathcal{O}_n^+) = \frac{\text{vol}(M_n)}{8n} = f(n)$ and $\text{vol}(\mathcal{O}_m^+) = \frac{\text{vol}(M_m)}{8m} = f(m)$. By Lemma 6.2, we know that $f(n)$ is strictly increasing, and so, we have that $\text{vol}(\mathcal{O}_n^+) \neq \text{vol}(\mathcal{O}_m^+)$, whenever $n \neq m$. Thus, \mathcal{O}_n^+ and \mathcal{O}_m^+ are non-isometric, whenever $n \neq m$. Since this minimal orbifold is unique for each non-arithmetic commensurability class, this implies that M_n and M_m are not commensurable if $n \neq m$.

Case 2: Now, suppose M_n and M_m are both arithmetic. Then from Theorem 1.1, we know that $m, n \in \{3, 4\}$. Proposition 4.1 implies that M_3 and M_4 have different invariant trace fields, and so, they must belong to different commensurability classes.

Case 3: Suppose M_n is arithmetic, while M_m is non-arithmetic. Since arithmeticity is a commensurability invariant, M_n is not commensurable with M_m .

Thus, we have that M_n is not commensurable to M_m , whenever $m \neq n$. The extension to half-twist partners follows from Proposition 3.2. \square

7. Half-twist partners with many hidden symmetries

Here, we will analyze a special subclass of half-twist partners of pretzel FALs. Consider the pretzel FAL \mathcal{P}_n and build its half-twist partner $\mathcal{P}'_n = \mathcal{P}_n(0, 1, 1, 1, \dots, 1)$. See the left side of Figure 13 for the pretzel FAL diagram of \mathcal{P}'_5 . In general, \mathcal{P}'_n has n crossing circles and 1 knot circle. In

addition, there is always exactly one untwisted crossing circle and $n - 1$ twisted crossing circles in \mathcal{P}'_n . Set $M'_n = \mathbb{S}^3 \setminus \mathcal{P}'_n$.

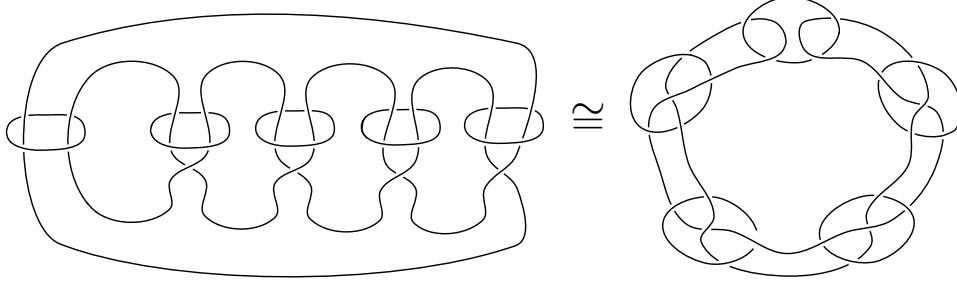


FIGURE 13. Two link diagrams of \mathcal{P}'_5 .

Our main goal for this section is to show that each non-arithmetic M'_n admits exactly $2n$ hidden symmetries, allowing us to construct non-arithmetic hyperbolic link complements with as many hidden symmetries as we would like, by taking n sufficiently large. To accomplish this goal, we first determine $\text{Sym}(M'_n)$. Similar to Section 6, we start by identifying a visually obvious subgroup of symmetries of $(\mathbb{S}^3, \mathcal{P}'_n)$ and then work to show this group must generate the full symmetry group $\text{Sym}(M'_n)$. However, unlike in Section 6, we can no longer use the fact that the quotient of M'_n by this visually obvious subgroup of symmetries gives a small volume orbifold. Instead, we will analyze how cusps intersect certain totally geodesic surfaces in M'_n in order to limit the number of symmetries of M'_n . From here, we can indirectly use our work from Section 6 to determine the number of hidden symmetries of M'_n .

By examining the diagram on the right side of Figure 13, we can see that $(\mathbb{S}^3, \mathcal{P}'_n)$ admits three order two symmetries: 180° rotation about the circular axis cutting through all of the half-twists (similar to the symmetry β in Figure 12), 180° rotation about the line L going through the middle of the untwisted crossing circle and the center of this ring of links, and the reflection in the vertical plane containing L .

Theorem 7.1. *$\text{Sym}(M'_n) \cong \mathbb{Z}/2\mathbb{Z} \times \mathbb{Z}/2\mathbb{Z} \times \mathbb{Z}/2\mathbb{Z}$, generated by the symmetries mentioned above.*

The proof of Theorem 7.1 requires some technical lemmas describing how symmetries of M'_n could act on its cusps. We now proceed to state and prove these lemmas before returning to the proof of Theorem 7.1.

By abuse of notation, let C denote both the untwisted crossing circle of \mathcal{P}'_n and the corresponding cusp of M'_n .

Lemma 7.2. *Let $\rho \in \text{Sym}(M'_n)$. Then ρ maps the cusp C to itself.*

Proof. A symmetry ρ can not map C to a cusp coming from a crossing circle with half-twists since they have different cusp shapes; see Proposition

2.6 and Lemma 2.7 for cusp shape descriptions. Now, we just need to show C can not map to the knot circle cusp. A nice description of how to build the boundary torus of a knot circle cusp for a FAL complement is given in Lemma 2.3 and Lemma 2.6 of [14]. In particular, the larger the number of crossing circles a knot circle goes through, the longer the longitude of this cusp (relative to its meridian). In our case, our knot circle goes through all n crossing circles twice, and so, a direct application of [14, Lemma 2.6] shows that the length of the longitude of this knot circle cusp is at least $2n$, while its meridian is length exactly 2 (for a particular horoball expansion). At the same time, since the cusp shape of C is $2\cos(\pi/n)i$, the ratio of the meridian to the longitude for C is at most two-to-one. Thus, C could not map to the knot circle cusp. \square

Choose a cusp expansion for M'_n and let $[\mu]$ and $[\lambda]$ denote the isotopy classes of the meridian and longitude, respectively, on the boundary torus ∂C . When we refer to the length of an isotopy class of a closed geodesic on ∂C , we mean the length of a geodesic representative.

Lemma 7.3. *Let $\rho \in \text{Sym}(M'_n)$. Then $\rho([\mu]) = \pm[\mu]$ and $\rho([\lambda]) = \pm[\lambda]$.*

Proof. Given $\rho \in \text{Sym}(M'_n)$, we know that ρ maps C to C from Lemma 7.2. Since ρ is an isometry, it must map geodesics on the torus ∂C to geodesics on ∂C with the same length. Choose the cusp expansion for C so that $[\mu]$ has length 1 and $[\lambda]$ has length $|2\cos(\pi/n)|$, as done in the proof of Proposition 2.6. Recall that all geodesics on the torus ∂C are of the form $k_1 \cdot \pm[\mu] + k_2 \cdot \pm[\lambda]$ for some integers $(k_1, k_2) \neq (0, 0)$. Since $1 < |2\cos(\pi/n)|$, we must have $\rho([\mu]) = \pm[\mu]$. Similarly, since $1 < |2\cos(\pi/n)| < 2$, we must have that $\rho([\lambda]) = \pm[\lambda]$. \square

The above lemma only tells us that given any fixed cusp expansion, the isotopy classes of the meridian and longitude must map to themselves. We would now like to place stronger restrictions on where particular geodesic representatives for $[\mu]$ and $[\lambda]$ could be mapped to under a symmetry of M'_n .

Now let D be the untwisted crossing disk that C bounds, and let W be the reflection surface in M'_n resulting from gluing the white faces of P_{\pm} . We wish to show D and W are each fixed set-wise by $\text{Sym}(M'_n)$.

The main tool is an analysis of intersecting embedded totally geodesic surfaces, particularly when one of them is a thrice-punctured sphere. Some preliminary observations are in order. An embedded totally geodesic surface in a hyperbolic 3-manifold lifts to a union of disjoint planes in the universal cover. Consequently, embedded totally geodesic surfaces intersect in a collection of pairwise disjoint simple geodesics. There are six simple geodesics on a thrice-punctured sphere, three joining distinct cusps (*intercusp* geodesics labeled a, b, c in Figure 14(a)) and three from a cusp to itself (*intracusp* geodesics labeled x, y, z in Figure 14(a)). Figure 14(b) displays these geodesics on a lift \tilde{D} to a fundamental region for D in $P_+ \cup P_-$. Any

embedded totally geodesic surface that intersects D must intersect D in a pairwise disjoint subset of these geodesics.

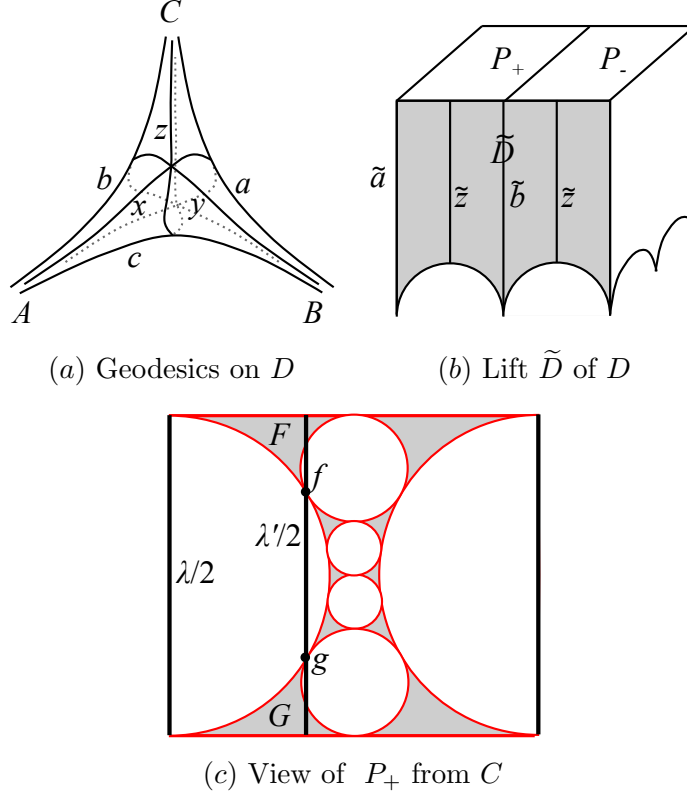


FIGURE 14. Totally geodesic surfaces

Further, any thrice-punctured sphere can be decomposed into two ideal triangles by slicing along intercusp geodesics. Let T denote such a triangle, then the simple geodesics of the thrice-punctured sphere intersect T in one of two ways. By construction, the edges of T correspond to intercusp geodesics. The intracusp geodesics are *midpoint rays*, i.e. hyperbolic rays perpendicular to one side of T and pointing toward the opposite vertex. The intracusp geodesic labeled \tilde{z} in Figure 14(b) demonstrates this phenomenon. Since T is a subset of the thrice-punctured sphere, any embedded totally geodesic surface intersects the triangle T in a pairwise disjoint collection of edges and midpoint rays. This significantly restricts how lifts of these surfaces intersect in the universal cover, a fact which we will use to our advantage.

The fundamental region $P_+ \cup P_-$ can be chosen so that the cusp corresponding to the untwisted crossing circle C is at infinity. In this case, the shaded sides are standard fundamental regions for the thrice punctured

sphere D , and the simple geodesics on D adjacent to C lift to those labeled \tilde{a} , \tilde{b} and \tilde{z} in Figure 14(b) (the intracusp geodesic is the union of the two geodesic rays labeled \tilde{z}).

Lemma 7.4. *The crossing disk D is a fixed set of any symmetry of M'_n .*

Proof. Let ρ be a symmetry of M'_n . As above, place the cusp corresponding to C at infinity in the universal cover \tilde{M}'_n of M'_n . A horosphere centered at infinity intersects the fundamental region $P_+ \cup P_-$ in a rectangle R comprised of two rectangular tiles (the tile in P_+ for T_6 is depicted in Figure 14(c)).

Now $\tilde{D} \cap R$ forms a longitude λ for the cusp C (the curve $\lambda/2$ of Figure 14(c) represents half a longitude). By Lemmas 7.2 and 7.3, we know ρ fixes C and must take λ to a copy λ' of $\pm\lambda$. We let \tilde{D}' denote the lift of the thrice-punctured sphere $\rho(D)$ to P_\pm . Then \tilde{D}' intersects R in λ' , a parallel copy of λ . Once we show $\lambda' = \pm\lambda$ we will have that $\tilde{D} = \tilde{D}'$, proving that $D = D'$.

Suppose $\tilde{D} \neq \tilde{D}'$. We begin by showing there is, up to symmetry, only one possible λ' different from λ . If \tilde{D}' is different from \tilde{D} , then it lifts to a vertical plane through R , parallel to the shaded sides and perpendicular to the white sides. The curve λ' cannot go precisely through the middle of R , for then D' would have too many punctures. Thus \tilde{D}' would have to intersect the shaded triangles labeled F, G in Figure 14(c). Now triangles F, G project to (triangles in) thrice punctured spheres S_F, S_G in M'_n . By the remarks preceding the lemma, the curve $\tilde{D}' \cap F$ must be an edge or a midpoint ray of F . This implies $\tilde{D}' \cap F$ must go through the vertices labeled f, g in Figure 14(b). We now finish the contradiction by showing that area considerations prevent this case from happening.

We will show that for this λ' the area $\mathcal{A}(\tilde{D}')$ of \tilde{D}' is greater than 2π so that it can't be a thrice punctured sphere. Let $\tilde{D}'_+ = \tilde{D}' \cap P_+$ is as in Figure 14(c), and note that $\mathcal{A}(\tilde{D}') \geq 2\mathcal{A}(\tilde{D}'_+)$ because there is an identical copy of \tilde{D}'_+ in P_- , so it suffices to show $\mathcal{A}(\tilde{D}'_+) > \pi$. Since \tilde{D}'_+ is a polygon, its area is 2π less than the sum of the external angles, where the external angle of an ideal vertex is π . Now \tilde{D}'_+ has three ideal vertices (f, g and at the cusp C), and a finite vertex along each vertical edge of \tilde{D}'_+ . Summing the external angles gives a value strictly greater than 3π , proving that $\mathcal{A}(\tilde{D}'_+) > \pi$. Thus the assumption $\tilde{D}' \neq \tilde{D}$ is false, proving the lemma. \square

Lemma 7.5. *The reflection surface W is a fixed set of any symmetry of M'_n .*

Proof. Again let $\rho \in \text{Sym}(M'_n)$, and we wish to show $\rho(W) = W$. As in Figure 14(a), label the cusps of D by A, B , and C where C corresponds to the crossing circle cusp, and label the intercusp geodesics by a, b , and c . The reflection surface W has two components, both of which intersect D . One of the components, say U , of W has just the knot circle as boundary,

and can be thought of as obtained by attaching the inner and outer disks of the projection plane by one untwisted band through C and $n - 1$ half-twisted bands through the other crossing circles. Thus U intersects D in the geodesic c opposite C . The other component of W , denoted V , is punctured by C along two meridians, and intersects D in geodesics a and b .

Let U' and V' denote the images of U and V under ρ , respectively. The isometry ρ preserves the cusp C by Lemma 7.2, and the crossing disk D by Lemma 7.4. Thus it either fixes or swaps cusps A, B , and acts analogously on intercusp geodesics opposite the cusps. More precisely, ρ preserves the geodesic c , and the set $\{a, b\}$. This implies that $U' \cap D = c = U \cap D$ and $V' \cap D = \{a, b\} = V \cap D$. Moreover, ρ preserves angles so all the surfaces U, U', V, V' are orthogonal to D . Thus both U and U' are connected, embedded, totally geodesic surfaces that intersect D orthogonally in the geodesic c (and similarly for V, V' using geodesics $\{a, b\}$). Therefore both lift to the plane in P_+ containing \tilde{c} and orthogonal to \tilde{D} . Projecting back to M'_n shows that in fact $U = U'$ (similarly $V = V'$). Since $W = U \cup V$, the proof is complete. \square

Lemmas 7.4 and 7.5 allow us to determine the images of a longitude-meridian pair (λ, μ) under any symmetry of M'_n . The rectangle R in $P_+ \cup P_-$ projects to a torus boundary ∂C of the cusp C . The crossing disk D intersects ∂C in a longitude λ , and the reflection surface W intersects ∂C in two meridians we denote μ_1, μ_2 . Choosing $\mu = \mu_1$ and λ as our generators for $\pi_1 \partial(C)$ we can now explicitly determine their possible images under $Sym(M'_n)$.

Corollary 7.6. *If $\rho \in Sym(M'_n)$, then $\rho(\lambda) = \pm\lambda$ and $\rho(\mu) = \pm\mu_i$, for some $i \in \{1, 2\}$.*

Proof. Since D is fixed by ρ (Lemma 7.4), we have $D \cap N(C) = \lambda$ is fixed as well, or that $\lambda = \pm\lambda$. Lemma 7.5 shows that W is fixed by ρ , so $\rho(\mu) \in \rho(W) \cap N(C) = W \cap N(C)$. This implies $\rho(\mu) \in \{\pm\mu_1, \pm\mu_2\}$. \square

At this point, we are finally able to prove Theorem 7.1.

Proof of Theorem 7.1. Fix a cusp expansion for C . Since any symmetry of M'_n maps C to C , we can consider the homomorphism $f : Sym(M'_n) \rightarrow Sym(C)$ given by restriction. We claim that this homomorphism is injective. Let $\rho \in Sym(M'_n)$, and suppose ρ restricted to C is the identity. So, ρ will fix any given point in the interior of C along with a tangent frame at that point. Then Proposition A.2.1 in Benedetti–Petronio [6] implies that ρ must be the identity map. Thus, the kernel of f is trivial, making this homomorphism injective.

Now, Corollary 7.6 implies that $|Sym(C)| \leq 8$ since there are only 8 possible combinations for where λ and μ could map to under a symmetry, and these symmetries of C are completely determined by how they act on λ and μ . At the same time, we know that $|Sym(\mathbb{S}^3, \mathcal{P}'_n)| \geq 8$, since we have

already identified a set of symmetries of $(\mathbb{S}^3, \mathcal{P}'_n)$ that generates a group of order 8. Since f is injective, we now have that $8 \leq |\text{Sym}(\mathbb{S}^3, \mathcal{P}'_n)| \leq |\text{Sym}(M'_n)| \leq |\text{Sym}(C)| \leq 8$, giving the desired result. \square

Finally, we can prove the main result of this section. Recall that a hidden symmetry of a hyperbolic 3-manifold $M = \mathbb{H}^3/\Gamma$ is an element of $C(\Gamma)/N(\Gamma)$.

Theorem 7.7. *For $n \geq 5$, M'_n is a non-arithmetic hyperbolic 3-manifold with $2n$ hidden symmetries.*

Proof. For $n \geq 5$, $M_n = \mathbb{H}^3/\Gamma_n$ and $M'_n = \mathbb{H}^3/\Gamma'_n$ are in the same commensurability class (Proposition 3.2) and non-arithmetic (Theorem 1.1). Thus, they cover a common minimal orbifold $\mathcal{O}_n = M_n/C(\Gamma_n)$. In Section 6, we showed that M_n has no hidden symmetries and its (full) symmetry group has order $16n$. This implies that $[C(\Gamma_n) : \Gamma_n] = 16n$. Thus, the cover $M_n \rightarrow \mathcal{O}_n$ is degree $16n$, and since M_n and M'_n have the same volume, we also have that the cover $M'_n \rightarrow \mathcal{O}_n$ is degree $16n$. Now, Theorem 7.1 implies that $[N(\Gamma'_n) : \Gamma'_n] = |\text{Sym}(M'_n)| = 8$ and since $16n = [N(\Gamma'_n) : \Gamma'_n][C(\Gamma'_n) : N(\Gamma'_n)]$, we have that $[C(\Gamma'_n) : N(\Gamma'_n)] = 2n$. This implies that M'_n has $2n$ hidden symmetries, as needed. \square

Corollary 7.8. *The number of hidden symmetries of M'_n grows linearly with volume.*

Proof. Recall that $\text{vol}(M'_n) = \text{vol}(M_n) = 8n(\mathcal{L}(\frac{\pi}{4} + \frac{\pi}{2n}) + \mathcal{L}(\frac{\pi}{4} - \frac{\pi}{2n}))$, where $\mathcal{L}(\theta)$ denotes the Lobachevsky function. Since the Lobachevsky function is continuous, we can choose an arbitrarily small $\epsilon > 0$, so that for all n sufficiently large, we have

$$16n(\mathcal{L}(\frac{\pi}{4}) - \epsilon) \leq \text{vol}(M'_n) \leq 16n(\mathcal{L}(\frac{\pi}{4}) + \epsilon).$$

Let HS_n denote the number of hidden symmetries for M'_n . Since Theorem 7.7 tells us that M'_n has $2n$ hidden symmetries, the above inequality implies that

$$\frac{\text{vol}(M'_n)}{8(\mathcal{L}(\pi/4) + \epsilon)} \leq HS_n \leq \frac{\text{vol}(M'_n)}{8(\mathcal{L}(\pi/4) - \epsilon)}$$

which gives the desired bound. \square

Remark 1: Corollary 7.8 actually highlights the fastest growth rate for the number of hidden symmetries that any sequence of non-arithmetic hyperbolic 3-manifold can have relative to volume. To justify this, we give an upper bound. Given a non-arithmetic hyperbolic 3-manifold $M = \mathbb{H}^3/\Gamma$, the number of hidden symmetries of M is at most $[C(\Gamma) : \Gamma]$, with equality exactly when M admits no symmetries. At the same time, $[C(\Gamma) : \Gamma]$ also gives the degree of the cover $M \rightarrow \mathcal{O}$, where \mathcal{O} is the minimal orbifold in M 's commensurability class. Since $\text{vol}(\mathcal{O})$ is uniformly bounded below by the volume of the minimal volume hyperbolic 3-orbifold (say this has volume v_0), we have that any non-arithmetic M has at most $\text{vol}(M)/v_0$

hidden symmetries. Thus, given any sequence of non-arithmetic hyperbolic 3-manifolds, the number of hidden symmetries can grow at most linearly with volume.

Remark 2: In [23, Section 7], Millichap shows that if you perform sufficiently long Dehn fillings on all of the crossing circles of \mathcal{P}'_n (with n odd), then the resulting knot complement admits no hidden symmetries. It is interesting to see that even though \mathcal{M}'_n admits many hidden symmetries, performing long Dehn fillings will always break these hidden symmetries in these cases. In light of this fact and Theorem 1.2 from [10], it seems plausible that highly twisted knot complements (that come from performing sufficiently long Dehn fillings along crossing circles of a FAL with a single knot component) will admit no hidden symmetries.

References

- [1] ADAMS, C. Limit volumes of hyperbolic three-orbifolds. *J. Differential Geometry*. **34** (1991), no. 1, 115–141. [MR1114455](#) (92d:57029), [Zbl 0697.57007](#), doi:[10.4310/jdg/1214446993](#).
- [2] BACH, E.; SHALLIT, J. Algorithmic number theory. Vol. 1. Efficient algorithms *Foundations of Computing Series*. MIT Press, Cambridge, MA, 1996. [MR1406794](#) (97e:11157).
- [3] BAKER, M.D. Link complements and the Bianchi modular groups. *Trans. A. M. S.* **353** (2001), 3229–3246. [MR1695016](#) (2001j:57007), [Zbl 0986.20049](#), doi:[10.1090/S0002-9947-01-02555-7](#)
- [4] BAKER, M.D. All links are sublinks of arithmetic links. *Pacific J. Math.* **203** (2002), no. 2, 257–263. [MR1897900](#) (2003a:57008), [Zbl 1051.57007](#), doi:[10.2140/pjm.2002.203.257](#).
- [5] BAKER, M.D.; REID, A.W. Principal Congruence Link Complements. *Ann. Fac. Sci. Toulouse Math.* **23** (2014), no. 5, 1063–1092. [MR3294602](#), [Zbl 1322.57015](#), doi:[10.5802/afst.1436](#).
- [6] BENEDETTI, R.; PETRONIO, C. Lectures on hyperbolic geometry. *Universitext, Springer-Verlag*. Berlin (1992). [MR1219310](#) (94e:57015).
- [7] CALEGARI, D. Real places and torus bundles. *Geom. Dedicata*. **118** (2006), 209–227. [MR2239457](#) (2007d:57026), [Zbl 1420.57047](#), [arXiv:math/0510416](#), doi:[10.1007/s10711-005-9037-9](#).
- [8] CHAMPANERKAR, A.; KOFMAN, I.; PURCELL, J. Geometry of Biperiodic Alternating Links. *J. Lond. Math. Soc. (2)*. **99** (2019) no. 3, 807–830. [MR3977891](#), [Zbl 07079420](#), [arXiv:1802.05343](#), doi:[10.1112/jlms.12195](#).
- [9] CHESEBRO, E.; DEBLOIS, J. Hidden symmetries via hidden extensions. *Proc. Amer. Math. Soc.* **145**. **8** (2017), 3629–3644. [MR3652814](#), [Zbl 1379.57009](#), [arXiv:1501.00726](#).
- [10] CHESEBRO, E.; DEBLOIS, J.; MONDAL, P. Generic hyperbolic knot complements without hidden symmetries. Preprint, [arXiv:1910.04712](#).
- [11] CHESEBRO, E.; DEBLOIS, J.; WILTON, H. Some virtually special hyperbolic 3-manifold groups. *Comment. Math. Helv.* **87** (2012), no. 3, 727–787. [MR2980525](#), [Zbl 1283.57007](#), [arXiv:0903.5288](#), doi:[10.4171/CMH/267](#).
- [12] FLINT, R. Intercusp Geodesics and Cusp Shapes of Fully Augmented Links. *ProQuest LLC*. Ann Arbor, MI, 2017, Thesis (Ph.D.) - City University of New York. [MR3664936](#), [arXiv:1811.07397](#).

- [13] FORD, K. The number of solutions of $\phi(x) = m$. *Ann. of Math. (2)*. **150** (1999), no. 1, 283–311. [MR1715326](#) (2001e:11099), [Zbl 0978.11053](#), [arXiv:math/9907204](#), doi: [10.2307/121103](#).
- [14] FUTER, D.; PURCELL, J. Links with no exceptional surgeries. *Comment. Math. Helv.* **82** (2007), no. 3, 629–664. [MR2314056](#) (2008k:57008), [Zbl 1134.57003](#), [arXiv:math/0412307](#), doi: [10.4171/CMH/105](#).
- [15] HARNOIS, J.; OLSON, H.; TRAPP, R. Hyperbolic tangle surgeries and nested links. *Algebraic & Geometric Topology*. **18** (2018), no. 3, 1573–1602. [MR3784013](#), [Zbl 1396.57008](#), doi: [10.2140/agt.2018.18.1573](#).
- [16] HENRY, S.R.; WEEKS, J.R. Symmetry groups of hyperbolic knots and links. *J. Knot Theory Ramifications*. **1** (1992), no. 2, 185–201. [MR1164115](#) (93e:57007), [Zbl 0757.57008](#), doi: [10.1142/S0218216592000100](#).
- [17] JEON, B. Hyperbolic 3-manifolds of bounded volume and trace field degree. *ProQuest LLC, 2013*. Thesis (Ph.D.) - University of Illinois at Urbana-Champaign. [MR3218104](#).
- [18] LACKENBY, M. The volume of hyperbolic alternating link complements. *Proc. London Math. Soc. (3)* **88** (2004), no. 1, 204–224, With an appendix by Ian Agol and Dylan Thurston. [MR2018964](#) (2004i:57008), [Zbl 1041.57002](#), [arXiv:math/0012185](#), doi: [10.1112/S0024611503014291](#).
- [19] LEHMER, H. A note on trigonometric algebraic numbers. *American Mathematical Monthly*. **40** (1933), 165–166. [MR1522747](#), [Zbl 0063.00001](#), doi: [10.2307/2301023](#).
- [20] MACLACHLAN C.; REID, A.W. The Arithmetic of Hyperbolic 3-Manifolds. *Graduate Texts in Mathematics*, vol. 219, Springer-Verlag, New York, (2003). [MR1937957](#) (2004i:57021), [Zbl 1025.57001](#).
- [21] MARGULIS, G.A. Discrete subgroups of semisimple Lie groups. *Ergebnisse der Mathematik und ihrer Grenzgebiete (3)*. **17** Springer, 1991. [MR1090825](#) (92h:22021), [Zbl 0732.22008](#).
- [22] MARSHALL, T.H.; MARTIN, G.J. Minimal co-volume hyperbolic lattices, II: Simple torsion in a Kleinian group. *Ann. of Math. (2)*. **176** (2012), no. 1, 261–301. [MR2925384](#), [Zbl 1252.30030](#), doi: [10.4007/annals.2012.176.1.4](#).
- [23] MILLICHAP, C. Mutations and short geodesics in hyperbolic 3-manifolds. *Comm. Anal. Geom.* **25** (2017), no. 3, 625–683. [MR3702548](#), [Zbl 1385.57018](#), [arXiv:1406.6033](#), doi: [10.4310/CAG.2017.v25.n3.a5](#).
- [24] MILLICHAP, C.; WORDEN, W. Hidden symmetries and commensurability of 2-bridge link complements. *Pacific J. Math.* **285** (2016), no. 2, 453–484. [MR3575575](#), [Zbl 1361.57013](#), [arXiv:1601.01015](#), doi: [10.2140/pjm.2016.285.453](#).
- [25] NEUMANN, W. Realizing arithmetic invariants of hyperbolic 3-manifolds. *Interactions between hyperbolic geometry, quantum topology and number theory*. 233–246, *Contemp. Math., Amer. Math. Soc., Providence, RI* **541**, (2011). [MR2796636](#) (2012e:57030), [Zbl 1237.57013](#), [arXiv:1108.0062](#), doi: [10.1090/conm/541](#).
- [26] NEUMANN, W.; REID, A.W. Arithmetic of hyperbolic manifolds. *Topology '90* (Columbus, OH, 1990), *Ohio State Univ. Math. Res. Inst. Publ., vol. 1, de Gruyter, Berlin*, 1992, 273–310. [MR1184416](#) (94c:57024), [Zbl 0777.57007](#).
- [27] NEUMANN, W.; TSVIETKOVA, A. Intercusp geodesics and the invariant trace field of hyperbolic 3-manifolds. *Proc. Amer. Math. Soc.* **144** (2016), no. 2, 887–896. [MR3430862](#), [Zbl 1360.57020](#), [arXiv:1402.5582](#), doi: [10.1090/proc/12704](#).
- [28] PURCELL, J. *An introduction to fully augmented links*. Interactions between hyperbolic geometry, quantum topology and number theory. 205–220, *Contemp. Math., Amer. Math. Soc., Providence, RI* **541**, (2011). [MR2796634](#) (2012c:57019), [Zbl 1236.57006](#), doi: [10.1090/conm/541](#).
- [29] PURCELL, J. *Hyperbolic geometry of multiply twisted knots*. *Communications in Analysis and Geometry*. **18** (2010), no. 1, 101–120. [MR2660459](#) (2012b:57040), [Zbl 1213.57016](#), [arXiv:0709.2919](#), doi: [10.4310/CAG.2010.v18.n1.a4](#).

- [30] PURCELL, J. *Slope lengths and generalized augmented links*. Communications in Analysis and Geometry. **16** (2008), no. 4, 883–905. [MR2471374](#) (2009k:57014), [Zbl 1171.57009](#), [arXiv:math/0703638](#) doi: [10.4310/CAG.2008.v16.n4.a7](#).
- [31] PURCELL, J. *Volumes of highly twisted knots and links*. Algebraic & Geometric Topology. **7** (2007), 93–108. [MR2289805](#) (2007m:57011), [Zbl 1135.57005](#), [arXiv:math/0604476](#), doi: [10.2140/agt.2007.7.93](#).
- [32] REID, A.W.; WALSH, G. *Commensurability classes of 2-bridge knot complements*. Algebraic & Geometric Topology. **8** (2008), no. 2, 1031–1057. [MR2443107](#) (2009i:57020), [Zbl 1154.57001](#), [arXiv:math/0612473](#), doi: [10.2140/agt.2008.8.1031](#).
- [33] THURSTON, W. *The Geometry and Topology of 3-Manifolds*. Lecture Notes, Princeton University Math. Dept. (1978).
- [34] THURSTON, W. *Three-dimensional manifolds, Kleinian groups and hyperbolic geometry*. Bull. Amer. Math. Soc. (N.S.) **6** (1982), no. 3, 357–381. [MR0648524](#) (83h:57019), [Zbl 0496.57005](#), doi: [10.1090/S0273-0979-1982-15003-0](#).
- [35] WALSH, G.S. *Orbifolds and commensurability*. Interactions between hyperbolic geometry, quantum topology and number theory. 221–231, Contemp. Math., Amer. Math. Soc., Providence, RI **541**, (2011). [MR2796635](#) (2012e:57048), [Zbl 1231.57017](#), [arXiv:1003.1335](#), doi: [10.1090/conm/541](#).
- [36] WATKINS, W.; ZEITLIN, J. *The minimal polynomial of $\cos(2\pi/n)$* . Amer. Math. Monthly **100** (1993), no. 5, 471–474. [MR1215534](#) (94b:12001), [Zbl 0796.11008](#), doi: [10.2307/2324301](#).

DEPARTMENT OF MATHEMATICS, CALIFORNIA STATE UNIVERSITY, SAN BERNARDINO,
CA 92407
jeffrey.meyer@csusb.edu

DEPARTMENT OF MATHEMATICS, FURMAN UNIVERSITY, GREENVILLE, SC 29613
Christian.Millichap@furman.edu

DEPARTMENT OF MATHEMATICS, CALIFORNIA STATE UNIVERSITY, SAN BERNARDINO,
CA 92407
rtrapp@csusb.edu